Journal of Hydrology 615 (2022) 128711

Contents lists available at ScienceDirect

Journal of Hydrology

journal homepage: www.elsevier.com/locate/jhydrol

Research papers

The cold regions hydrological modelling platform for hydrological diagnosis and prediction based on process understanding

J.W. Pomeroy [a,*], T. Brown [a,b], X. Fang [a], K.R. Shook [a], D. Pradhananga [c], R. Armstrong [d], P. Harder [a], C. Marsh [a], D. Costa [e], S.A. Krogh [f], C. Aubry-Wake [a], H. Annand [a], P. Lawford [a], Z. He [a], M. Kompanizare [a], J.I. Lopez Moreno [g]

[a] Centre for Hydrology, University of Saskatchewan, Saskatoon and Canmore, Canada
[b] Rowan Systems, Saskatoon, Canada
[c] Tribhuvan University, Nepal
[d] University of Queensland, Australia
[e] Environment and Climate Change, Canada
[f] Department of Water Resources, Faculty of Agricultural Engineering, University of Concepción, Chillán, Chile
[g] Pyrenean Institute of Ecology-CSIC. Zaragoza, Spain

A R T I C L E I N F O

This manuscript was handled by Marco Borga, Editor-in-Chief, with the assistance of Francesco Avanzi, Associate Editor

Keywords:
Snow
Frozen ground
Evapotranspiration
Water quality
Glaciers
Hydrological modelling

A B S T R A C T

Cold regions involve hydrological processes that are not often addressed appropriately in hydrological models. The Cold Regions Hydrological Modelling platform (CRHM) was initially developed in 1998 to assemble and explore the hydrological understanding developed from a series of research basins spanning Canada and international cold regions. Hydrological processes and basin response in cold regions are simulated in a flexible, modular, object-oriented, multiphysics platform. The CRHM platform allows for multiple representations of forcing data interpolation and extrapolation, hydrological model spatial and physical process structures, and parameter values. It is well suited for model falsification, algorithm intercomparison and benchmarking, and has been deployed for basin hydrology diagnosis, prediction, land use change and water quality analysis, climate impact analysis and flood forecasting around the world. This paper describes CRHM's capabilities, and the insights derived by applying the model in concert with process hydrology research and using the combined information and understanding from research basins to predict hydrological variables, diagnose hydrological change and determine the appropriateness of model structure and parameterisations.

1. Introduction

Cold regions, where snow and ice play an inordinately important role in streamflow generation, involve hydrological processes that are not often addressed appropriately in hydrological models (Wheater et al., 2022). Many cold regions are also sub-humid and so have the added complication of seasonal aridity (Armstrong et al., 2010). Since most cold regions have been glaciated in recent geological time, geomorphological processes have not always had sufficient time to develop well-defined drainage networks and stream channels and so depressional storage capacities are large and the runoff contributing areas for streamflow generation are variable (Shook et al., 2015). In mountains, snowpacks can cover the basin for more than 2/3 of the year and in some areas, year-round, as permanent snowfields and glaciers that dominate the coldest and snowiest parts of high mountain basins (Pomeroy et al., 2012a; Fang & Pomeroy, 2020; Pradhananga & Pomeroy, 2022). Cold regions, including snowy, sub-humid and sparsely or ungauged basins pose special challenges to hydrological prediction due to the need to address snow and ice processes such as snow redistribution and ablation and infiltration to frozen soils, strong seasonality in process operations, bidirectional phase changes from water to vapour, ice to liquid and ice to vapour, variable contributing area, episodic flow processes, and restricted opportunity to calibrate model parameters from streamflow observations due to intermittent streamflow, small contributing areas to streamflow, and lack of gauging stations (Pomeroy et al., 1998a; Pomeroy et al., 2007, Shook et al., 2021).

* Corresponding author at: Centre for Hydrology, Dept. of Geography & Planning, University of Saskatchewan, 101 – 121 Research Drive, Saskatoon, Saskatchewan S7N 1K2, Canada.
E-mail address: john.pomeroy@usask.ca (J.W. Pomeroy).

https://doi.org/10.1016/j.jhydrol.2022.128711
Received 5 May 2022; Received in revised form 1 October 2022; Accepted 16 October 2022
Available online 8 November 2022

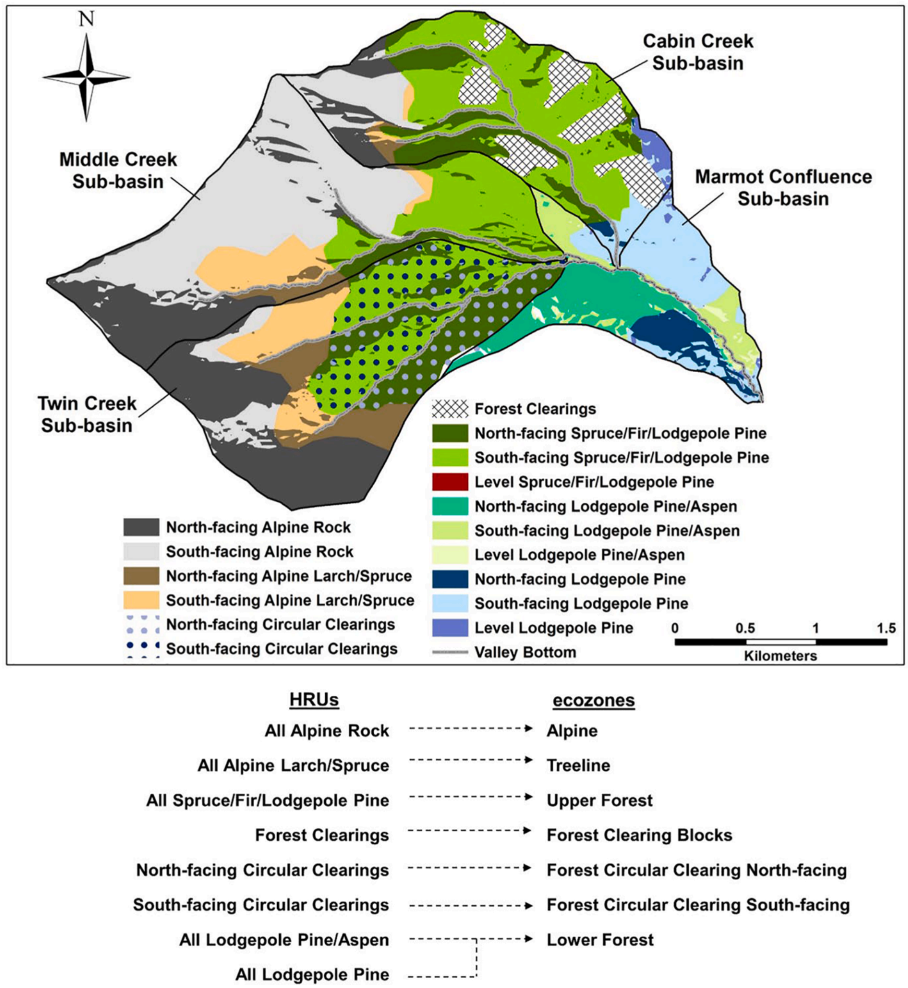

Fig. 1. HRUs map, sub-basins and ecozones used to discretize Marmot Creek Research Basin, Alberta, Canada (Fang & Pomeroy, 2020). Note that the size and areas of circular clearings in Twin Creek Sub-basin are not to scale.

Solutions to these challenges have required half a century of intensive cold regions and sub-humid zone process hydrology investigations in Western Canada and development of alternatives to model calibration from local streamflow to develop functional modelling systems (Pomeroy et al., 2004; Pomeroy et al., 2007; Pomeroy et al., 2013). These process studies began in research basins established during the UNESCO International Hydrological Decade of 1965–75 in the semi-arid, continental climate of the Canadian Prairies – an agricultural region with a landscape dominated by annual cereal and oil seed production interspersed with perennial pastures having very mild topography and incomplete drainage basin development leading to vast areas with no streams (Gray & Granger, 1988). Here, blowing snow transport and sublimation dominate the winter redistribution of snow, soils freeze to depths of greater than 1.5 m with limited infiltration capacities, snowmelt occurs over a few weeks or less controlled by solar irradiance, and snowmelt contributing to over 85 % of annual streamflow (Gray et al., 1986). After snowmelt, evapotranspiration normally exceeds spring and summer precipitation, soils thaw and infiltration capacities are large and so runoff events are restricted to intense rainstorms, usually due to convective precipitation or infrequent, large multi-day storms that saturate the soils (Dyck et al., 1974; Granger & Gray, 1989). Streamflow is only generated after surface depressional storage is filled and "fill and spill" runoff generation can be initiated when water levels in depressions exceed sill levels as originally proposed by Chris Spence (Spence et al., 2022; Pomeroy et al., 2010). These studies led to several realisations that showed the inadequacy of hydrological modelling at the time; the need to model basins without identifiable streams, the need to include a full range of snow and frozen ground processes, the need to parameterize a model without calibration of parameters to observed streamflow, the need to calculate net radiation as a fundamental driver of coupled heat and mass transfer calculations, and the need to treat landscape units as a natural, fundamental spatial basis for discretization of basins for water balance calculations. Research in other basins in northern Canada and the Canadian Rockies revealed the importance of permafrost, glaciers, forests and shrubs to the hydrology of these regions (Bash & Marshall, 2014; Connon et al., 2014; Ménard et al., 2014; Quinton & Baltzer, 2013; Nicholls & Carey, 2021; Pomeroy et al., 2012a; Pradhananga & Pomeroy, 2022).

The inability of models developed in temperate parts of the world to successfully simulate the hydrology of cold regions, led to the development of the Cold Regions Hydrological Modelling platform (CRHM, Pomeroy et al., 2007), to simulate how cryospheric and hydrological processes govern basin hydrology by linking the energy and mass balance equations together via phase change in a flexible, modular predictive framework. The model distributes the forcing meteorology to appropriate hydrologically meaningful landscape units that serve as control volumes for hydrological process calculations, and which can be aggregated to calculate streamflow at multiple scales. Modules can be coupled in a wide variety of ways to represent alternative spatial structures, or forcing meteorology, or processes and process algorithms – this permits the rapid development of many models from the platform. CRHM was designed to test multiple hypotheses about model structure,

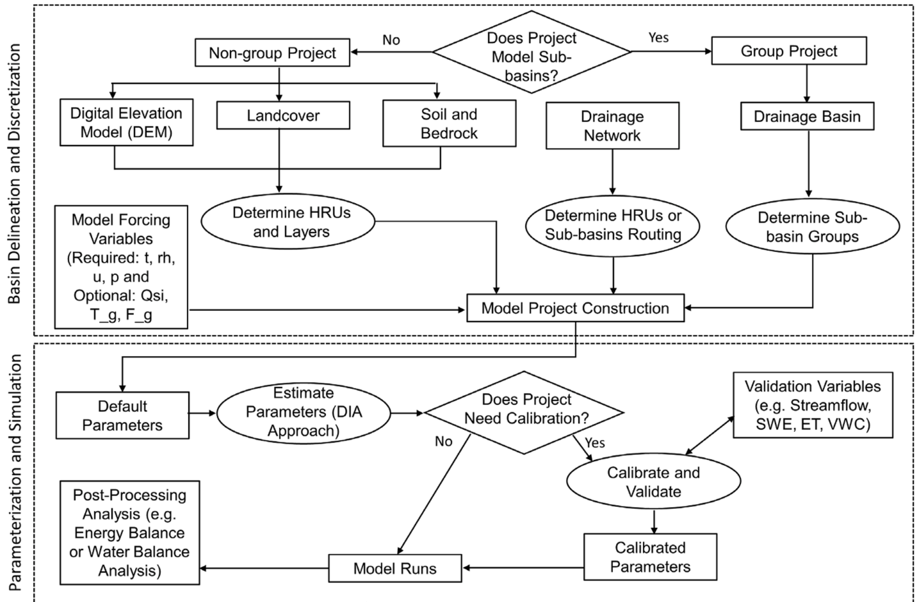

Fig. 2. CRHM model workflow. DIA Approach refers to the Deduction, Induction and Abduction approach to model parameterisation for ungauged basins by Pomeroy et al. (2013).

process description and inclusion, and algorithm integrity, and to output any hydrological variable in a practical and easy to use system. It has been used in model falsifications to diagnose suitable model scale, structure and process capabilities (Dornes et al., 2008; Fang et al., 2013a,b; Lv et al., 2019).

The intention of CRHM's development has been to couple model development and application to process hydrology investigations in research basins to examine process importance and algorithm appropriateness for describing cold regions hydrology and to use the model as a tool, in combination with field investigations, to diagnose hydrological functioning of basins and their sensitivity to land use and climate change. The model has been further developed since 2007 for forest, permafrost, wetland, mountain, and glaciated basins and to predict water quality and hydrology. It has been applied on every continent except Antarctica and redesigned to calculate hydrological fluxes over larger river basins (Cordeiro et al., 2017; Costa et al., 2021; Fang et al., 2010, 2013; He et al., 2021; Krinner et al., 2018; Krogh et al., 2015; Krogh & Pomeroy, 2018; López-Moreno et al, 2013, López-Moreno et al., 2016, López-Moreno et al., 2017; Pomeroy et al., 2013; Pradhananga & Pomeroy, 2022; Rasouli et al., 2014, 2019,2022; Sanmiguel-Vallelado et al., 2022; Stone et al., 2019; Van Hoy et al., 2020; Weber et al., 2016; Zhou et al., 2014). These versions have been used to study snowmelt and glacier contributions to streamflow, summer evapotranspiration and soil moisture regimes, drought, excess nutrient runoff, forest hydrology, climate change impacts, agricultural land management strategies, frozen ground impacts on hydrology and climate and vegetation change impacts on permafrost. CRHM has been operationalized in flood forecasting systems (Pomeroy et al., 2013) and used to inform the development of continental scale models such as MESH, CLASS and CHM (Marsh et al., 2020; Wheater et al., 2022). However, the uniqueness of the platform is its use as a tool for the hydrologist to deploy knowledge gained in field investigations to explore and diagnose hydrological functioning from hydrological processes up to streamflow generation in basins in a systematic way. The advantage of the typically uncalibrated approach with CRHM is in learning from model failure, through model falsification or from learning from changing model performance as discretization, modules and parameters are changed. This has been detailed in papers such as Armstrong et al., 2009; Dornes et al., 2008; Fang et al. (2013a,b); Pomeroy et al., (2013; Pomeroy et al., 2016a). This experience has helped inform research directions and algorithm improvements. For instance, the failure of ET-soil moisture coupling algorithms in severe drought and extreme wet conditions in the Canadian Prairies was particularly instructive (Armstrong et al., 2010; Mahmood et al., 2017).

The purpose of this paper is to describe CRHM's capabilities and the insights derived from using the model along with process hydrology research, to diagnose hydrological change and the appropriateness of model structure and parameterisation. It focusses on developments, diagnoses and applications since the publication of an extensive description of CRHM by Pomeroy et al. (2007) 15 years ago and provides an example of the fusion of hydrological process research, field observations and modelling that has provided new understanding and capabilities for modelling hydrology and water quality in cold regions and elsewhere.

2. Model structure

In CRHM, the user constructs a purpose-built model from a selection of possible basin spatial configurations, spatial resolutions, and physical process modules of varying degrees of physical complexity. Basin discretization is performed via hydrological response units (HRUs) whose number and nature are selected by the user based on the variability of basin attributes and the desired level of physical complexity. An example of basin discretization into HRU from ecozones, elevation, topography and hydrography is shown for Marmot Creek Research Basin in the Canadian Rockies as Fig. 1.

HRUs can interact with each other in several ways. Blowing snow, runoff and groundwater can flow amongst HRUs in different directions depending on surface aerodynamics and prevailing wind directions for blowing snow, aquifer characteristics and potential energy gradients for groundwater and gravity, and surface characteristics for runoff. Blowing snow can enter and leave a basin whilst groundwater and runoff are aggregated and routed as streamflow which can only leave a basin at the outlet. HRU assemblages for a basin can be grouped and declared a 'representative basin' which can then be repeated and adjusted to allow for rapid parameterisation of larger basins composed of many sub-basins (Fig. 1). A full and up-to-date description of the CRHM software and its installation can be found on the CHRM Wiki page which can be found here https://wiki.usask.ca/display/CRHMdoc/CRHM+-+Cold+Region+Hydrological+Model and on the CRHM website https://research-g

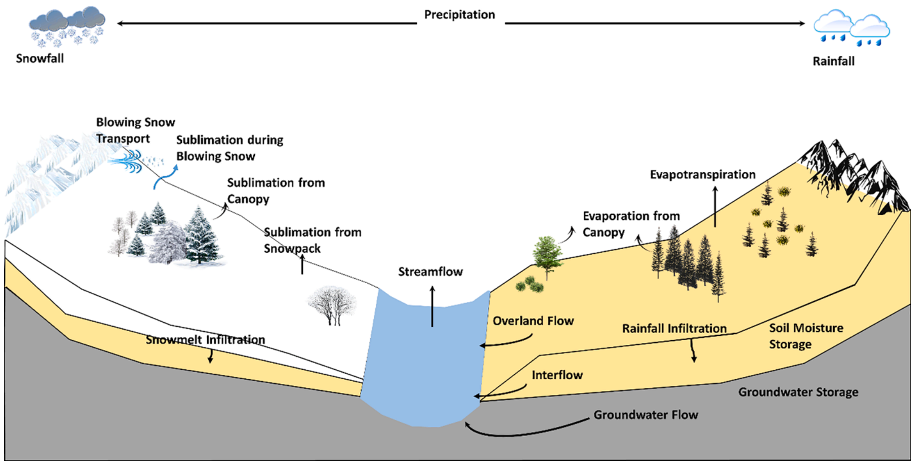

Fig. 3. Example of CRHM processes for a mountain basin, showing snow processes on the left-hand side and water flow processes and summer processes on the right-hand side.

roups.usask.ca/hydrology/modelling/crhm.php with supporting R code described here https://research-groups.usask.ca/hydrology/modelling/r-packages.php.

CRHM was originally developed as an object-oriented modular modelling platform in 1998 using the Borland C++ compiler and included a dynamic linked library version (DLL) that was distributed to module developers in the UK and Canada. Many modules were developed based on research in the University of Saskatchewan's Division of Hydrology, Environment Canada's National Hydrology Research Institute and the University of Wales, Aberystwyth. Each CRHM release version was numbered and dated as were all modules and all modules were reviewed before inclusion. With the demise of Borland and the inability of users to purchase its C++ compiler, the development of CRHM had to be centralized and carefully controlled. This was done with a small group of scientists working with the CRHM code developer, Tom Brown, in informal and formal discussions, often in sessions in Saskatoon beverage rooms. Modules were conceptualized, debated, reviewed and added, and model users could request new modules on request and review by this small group. Detailed help files were written and updated. The refactored version of CRHM that has just been released permits anyone to compile it with the GNU compiler connection (GCC) C++ and module developments are welcome and will be reviewed by the authors of this paper as part of a more formal version control process.

Modules are executed within HRUs and there is complete flexibility in defining and selecting HRUs – a model can be lumped with one HRU per sub-basin, fully distributed with many HRUs on a fine grid, or more typically, semi-distributed where HRUs are landscape units that are assumed to have some common biogeophysical characteristics and hydrological drainage characteristics and therefore a single set of parameters. Intrinsic length scales of HRUs are that they should be large enough to avoid self-similarity in soil moisture and snow water equivalent (SWE), so at least 100 m (Shook and Gray, 1997) and less than about 3 km to ensure similar inputs from precipitation and snow redistribution and to calculate runoff (Dornes et al., 2008). Time steps for calculations in the HRU are set by observations and are assumed to be close to hourly. Modules may be grouped together to repeat the model structure in many sub-basins. Fig. 2 shows a general workflow for model development in CRHM based on several steps: 1) basin delineation and discretization (top panel), and 2) parameterization 3) simulation and 4) post-processing (bottom panel). For a non-group project, the basin delineation and discretization use geospatial datasets (i.e., DEM, landcover, soil and bedrock) to determine HRUs and soil or glacier firn layers. Group projects using basin discretization, require delineation of sub-basin groups. The parameters defining the routing length, gradients and sequences of HRUs and sub-basins are set based on datasets of stream networks. Basin delineation is often informed by GIS programs but can now be automated using tools such as the functions in R package CSHShydRology (https://cran.r-project.org/package=CSHShydRology).

Parameter values are rarely calibrated for CRHM models. Instead, parameter values are usually estimated based on the deduction, induction and abduction (DIA) approach which is suited for either gauged or ungauged basins (Pomeroy et al., 2013). Once parameter values are determined they can be written to CRHM model project (.prj) files using functions in CRHMr. Historically, most CRHM modelling has used data from meteorological stations as the source of forcing data. These data generally require considerable quality control, interpolation and extrapolation to make them suitable for forcing models. Pre-processing for CRHM models can be done using CRHMr which includes functions for data quality analyses and for infilling missing/bad values through interpolation and/or imputation. The package functions can write data in the observation file (.obs) formats used by CRHM. CRHM was originally a Windows program requiring a Graphic User Interface (GUI) that permits intuitive assembly of modules for model creation, HRU delineation, parameter setting, order of operation modification, and diagnostic model graphics and outputs and links to the help file. However, the recent refactoring of the program has allowed it to also be compiled as a command-line program, which enables it to be run on high performance computers . It has also resulted in the program running much faster. The CRHMr package contains functions to execute CRHM, of either version, and uses the Wine compatibility layer (https://www.winehq.org/) to run Windows-compatible executables on Linux or MacOS computers.

CRHM can output the values of almost any of hundreds of variable, which can result in very large output files. As many of the variables are used for internal purposes, their units may be difficult to work with. Although the output files are all simple text files, there can be many output formats depending on user needs. CRHMr contains functions to read any output file, and to post-process the values, including converting units and plotting time series of variables. There are also functions for performing water balances. Using R and CRHMr, the entire sequence of modelling in CRHM, can be automated, once the model structure, including the program modules and the number of HRUs has been decided on, and the initial.prj file has been created. The ability to parameterize and run models automatically aids the model reproducibility as all steps in the model development are recorded in the R code. Reproducibility has been shown to be crucial for the elevation of hydrological modelling to a more repeatable scientific endeavour (Knoben et al., 2021).

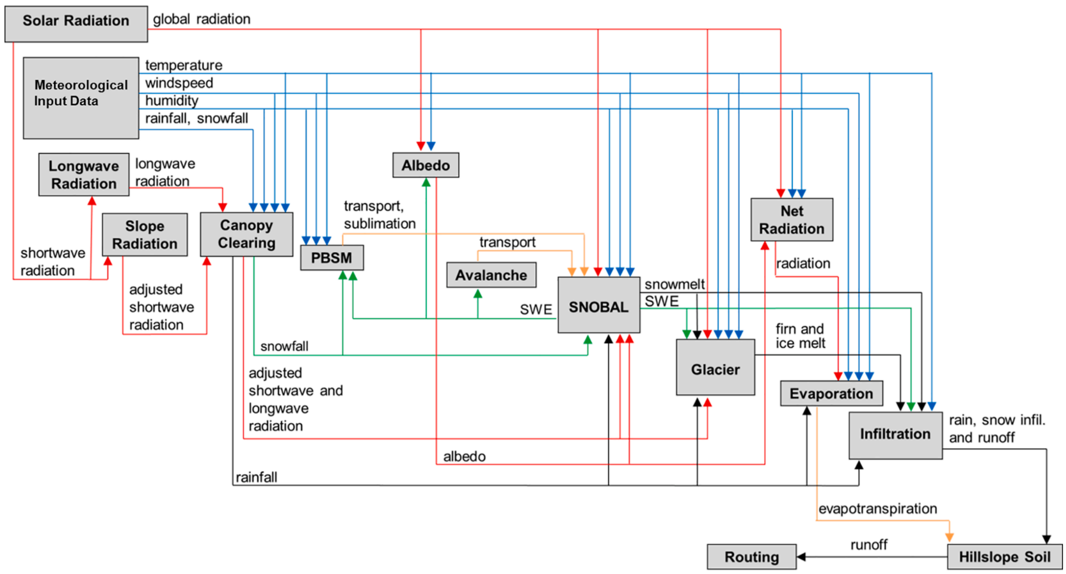

Fig. 4. Modular structure of CRHM – an example for a glacierized basin (Pradhananga & Pomeroy, 2022). Red linking arrows are radiation fluxes; blue arrows are meteorological forcing data; orange arrows are snow and water vapour mass transport; green and black arrows are model output state variables and fluxes.

3. Processes

3.1. Overview

Hydrological process modules in CRHM have been developed from the outcomes of intensive field and detailed modelling studies of cold regions and other hydrological processes. These modules can be specific to basin setup, such as delineating and discretizing the basin, conditioning observations for extrapolation and interpolation in the basin, or to hydrological calculation needs such as calculation of longwave radiation under forest canopies, wind flow over complex terrain, or snow albedo decay, but most commonly deal with hydrological processes such as evapotranspiration, infiltration, snowmelt, and streamflow discharge (Fig. 3 – model processes over a mountain basin). CRHM has a selection of process descriptions available at different levels of granularity as separate modules or as "variants" (options within a module) for each process and also the ability to rapidly create "macros" as new modules, on the fly to explore new hypotheses or algorithms. CRHM is unique in its range of cold regions hydrology and water quality capabilities, with strong physically based calculations of precipitation phase, snow redistribution by wind, snow interception, sublimation, sub-canopy radiation, snowmelt, glacier icemelt, icemelt under debris, snow avalanching, infiltration into frozen and unfrozen soils, hillslope water movement, frozen ground dynamics, actual evapotranspiration, lake evaporation, wetland fill and spill, soil water movement, subsurface preferential flow from tile drainage, groundwater flow, water chemistry and streamflow. It calculates runoff from rainfall and snowmelt as generated by infiltration excess and saturated overland flow, meltwater routing through glacier, flow over partially frozen soils, detention flow, shallow subsurface flow, preferential flow and groundwater flow. Water quality inputs to water bodies can also be simulated. The user selects the hydrological processes that they wish to simulate from over 97 modules and dozens of variants of these modules (https://wiki.usask.ca/display/CRHMdoc/CRHM+Module+Library). Some modules address a single process , with different algorithms, assumptions and data and parameter requirements, whilst other modules are more comprehensive dealing with, for example, all processes in snowpacks, glaciers or soils. There is also the capability to write a new module quickly using the "Macro" feature where the user writes a tentative module from within the platform. The Macro feature allows users to create simple modules suitable for testing algorithms and for diagnosing CRHM model output and is fully described here https://wiki.usask.ca/display/CRHMdoc/CRHM+Macros. Macros can also be used to create Groups for reproducing aspects of the model spatially (module sequences repeated in different sub-basins) https://wiki.usask.ca/display/CRHMdoc/Groups and Structures for intercomparing the performance of different groups of modules in an otherwise common model https://wiki.usask.ca/display/CRHMdoc/Structures which is useful in diagnosing different model structures. Macro modules that have proven successful or useful have been then converted into permanent modules in the platform. Whilst there is considerable freedom in these selections and end points, for instance a CRHM model can be configured only as a snow model, or an evapotranspiration model, or a soil moisture balance model, or as a full streamflow synthesis hydrology model, there are some modules that are required for almost all models, these modules deal with setting up the basin, inputting and adjusting observations to HRUs and calculation of radiation fluxes. An example of a CRHM model flow chart is shown in Fig. 4 for a partly glacierized mountain basin. Some of the principal modules are described in the following section.

Most modules have parameters that need to be specified and the physical basis of most modules means that most parameters are physically identifiable. CRHM was designed so that the user inputs parameters based on their knowledge of the basin, GIS and remote sensing analysis, soil surveys, digital elevation models, parameters that worked for similar process studies elsewhere or by borrowing parameters from other basins in similar hydroclimatic and ecological regions (Fig. 2). The deductive, inductive, and abductive (DIA) approach to parameterisation was described by Pomeroy et al. (2013) and is a recommended method that has shown to be successful in applying CRHM in and outside of research basins, including ungauged basins where parameter uncertainty is high. Many CRHM models provide reasonable simulations of snowpacks, soil moisture and streamflow using parameters set by the DIA approach without calibration of parameters from streamflow (Appendix, Table 1). However, some, particularly routing and subsurface parameters are difficult to observe, and so limited parameter calibration has been employed to improve streamflow synthesis.

3.2. Precipitation, meteorology, radiation, canopy adjustments

A critical aspect in successfully representing hydrological processes in any model is the treatment of the forcing meteorology. Assumptions around the extrapolation and interpolation of forcing data can therefore

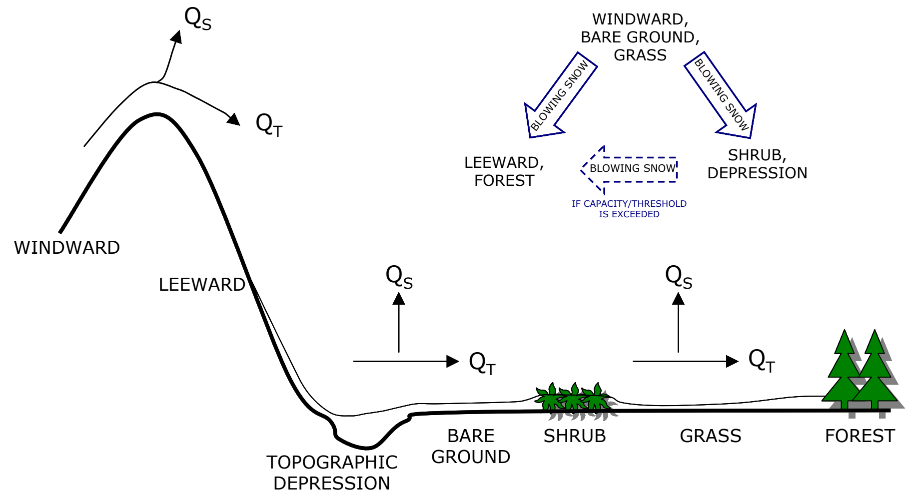

Fig. 5. Routing of blowing snow transport (Q_T) from HRU to HRU in vegetated and complex terrain and accompanying sublimation losses (Q_S) – a general approach employed in CRHM (MacDonald et al., 2009). Snow can only be transported from tall shrub or grass vegetation, once the exposed vegetation height is small enough to permit application of sufficient wind shear forces to erode snow and entrain it in the atmosphere.

have important implications for model performance. A comparison of commonly used precipitation phase partitioning approaches in CRHM demonstrated large changes in timing and magnitude of snow and streamflow generation processes over a variety of cold-regions research basins (Harder & Pomeroy, 2014). An obstacle to adoption of physically based process models has been the more complex forcing meteorological data requirements relative to the simpler requirement of conceptual or calibrated model approaches (Beven, 1993; Hrachowitz & Clark, 2017). The CRHM framework demonstrates that input data demands need not be onerous as a variety of physically guided approaches are employed to ingest, synthesize and distribute meteorological data to drive hydrological process representations and represent the climate perturbations necessary to answer research questions.

First order data requirements, from station, gridded observation, reanalysis, or climate model sources, include hourly observations of air temperature, relative humidity, wind speed, precipitation and incoming shortwave radiation. When radiation data are not available, CRHM uses methods described by Annandale et al. (2001) and Sicart et al. (2006) to simulate incoming shortwave and longwave radiation from air temperature and humidity data with relatively small errors. Forcing meteorology is distributed to HRUs by elevation, slope, aspect and location using user defined lapse rates to interpolate air temperature, humidity, and precipitation observations whilst respecting vapour pressure saturation limits. Air temperature and precipitation perturbation impacts on hydrological processes can be considered through simple delta change and multiplier functions (Gleick, 1986; Hay et al., 2000).

Hydrological process representations require a second order of information to account for the interactions of the meteorological data and the spatial variability of the basin and its land surface. Precipitation partitioning into rain or snow phases is critical in cold regions and the psychometric energy balance approach of Harder and Pomeroy (2013) is used to address the well documented dependence of phase upon temperature and humidity (Harpold et al., 2017; Jennings et al., 2018). In the absence of reliable humidity information, alternate approaches from air temperature (Harder & Pomeroy, 2014) and ice bulb temperature (Marks et al., 2013) thresholds are available. Wind induced gauge undercatch of snowfall is a persistent challenge in cold regions and is accounted for with Nipher (Goodison et al., 1998) and Alter-shielded corrections (Smith, 2009). The tight coupling of the water and energy balances when considering physical process representation requires detailed accounting of radiation variability and forest interactions. Basic corrections such as radiation correction for slope and aspect (Garnier & Ohmura, 1970) are applied at the HRU scale. Shortwave and longwave radiation transmissions are then simulated separately for effects of forest cover, accounting for differences amongst continuous forest canopies, forest gaps and larger clearings as functions of measurable forest parameters (Sicart et al., 2006; Pomeroy et al., 2009; Ellis et al., 2010). Wind flow over complex terrain is calculated using the parametric method of Walmsley et al. (1989), which adjusts wind speed for topographic location based on the results of a boundary layer model.

3.3. Snow redistribution and sublimation by wind, gravity and forest canopies

Snow redistribution by wind in open environments and by avalanches in steep mountain terrain are important processes for calculating the accumulation of the seasonal snowpack (Vionnet et al., 2021). CRHM calculates blowing snow transport and sublimation (Pomeroy, 1989; Pomeroy et al., 1993; Pomeroy and Gray, 1990; Pomeroy and Li, 2000; Pomeroy and Male, 1992; Pomeroy and Gray, 1995) to estimate HRU snowpack erosion and deposition as a mass balance of horizontal snow transport via saltation and suspension and in-transit sublimation using precipitation, wind speed, air temperature and relative humidity as well as information on the snowpack. Horizontal blowing snow redistribution by wind from one HRU to another is determined by considering exposed surface roughness as a function of snow depth and surface characteristics such as vegetation density and height. Snow can blow into a basin or sub-basin from outside of the basin, even if they are over a watershed divide. Three factors are needed for a blowing snow event to occur – wind speed greater than the threshold condition (Li & Pomeroy, 1997), friction from wind at the surface greater than that causing drag on exposed vegetation and bare ground (Pomeroy & Gray, 1994), and a supply of erodible snow or concurrent snowfall. Snow is eroded from wind-exposed HRUs and deposited as drifts in topographically sheltered or well vegetated HRUs. The blowing snow model in CRHM (Pomeroy et al., 2007) was extended to application of the model over mountains and complex terrain by MacDonald et al. (2009) using a parameterisation to transport snow from source to sink HRUs based on their exposed vegetation height and topographic position influencing relative wind speeds and shear stresses – this is shown in Fig. 5.

In addition to blowing snow, snow is redistributed by gravity in avalanches from higher to lower elevations on steep slopes, described by an avalanche module based on the algorithm developed by Bernhardt and Schulz (2010). Snow slides in an avalanche if the minimum snow holding depth and a minimum slope angle are exceeded. They suggested values of holding depth of 50 mm w.e. (water equivalent) and 25°

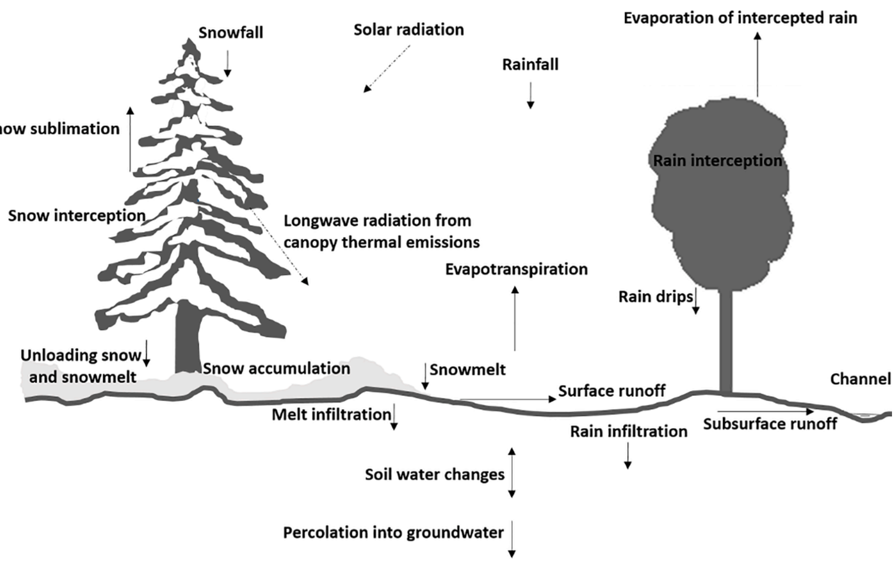

Fig. 6. Major hydrological processes in forest canopies and the sub-canopy environment that are represented in CRHM modules (adapted from Pomeroy et al., 1999, 2005).

minimum surface slope. For slopes steeper than the minimum slope angle, the snow holding depth decreases exponentially. This module moves snow downslope from steep HRUs to less steep HRUs. Importantly, it interacts with the blowing snow calculations. The blowing snow module will deposit snow in cornices at high elevation steep slope HRUs and the avalanche module will then redistribute this snow down the valley side, producing realistic high mountain snow distributions.

CRHM integrates a canopy module to represent the effects of forest canopy on snow, rainfall, sublimation, and evapotranspiration processes in a physically based manner (Fig. 6). Forest-precipitation interactions capture the interception of rainfall and snowfall in canopies to quantify evaporation and sublimation losses as a function of forest characteristics and snow unloading and drip as a function of ice bulb temperature (Hedstrom & Pomeroy, 1998; Ellis et al., 2010; Pomeroy et al., 1998b). In this module, snow interception is estimated by the antecedent canopy snow load, unloading rate coefficient, and maximum interception capacity of the canopy which is determined by the tree species, snowfall density and effective leaf area index (LAI) (Ellis et al., 2010). Canopy sublimation is estimated by multiplying the intercepted snow load by a physically based sublimation coefficient calculated from turbulent transfer of sensible heat to and water vapour away from an ideal ice sphere and then corrected for the degree of exposure of intercepted snow in the canopy as described by fractal geometry area-volume relationships (Pomeroy et al., 1998b). Under the canopy, snowmelt is governed by sub-canopy radiation and turbulent transfer relationships, and snowmelt and sub-canopy rainfall (including drip) connect to soil, infiltration and evapotranspiration modules and eventually to runoff routing modules (Figs. 3, 4, 6).

3.4. Energy for snowmelt, icemelt and sublimation

The energy available for snow, firn and ice melt and sublimation from the snow or ice surface is the sum of fluxes due to shortwave and longwave radiation, turbulent transfer of sensible heat, advection of energy from precipitation, internal energy state change in the snowpack and conduction of heat from the ground (Pomeroy et al., 1998a). Shortwave and longwave radiation are the principal sources of melt energy and the radiation module in CRHM simulates incoming shortwave (global) radiation adjusted to slope and aspect and so includes self-shading but not shadowing from surrounding topography. In the absence of observations, shortwave transmittance can be estimated using diurnal temperature ranges, latitude and time of year (Shook & Pomeroy, 2011a) and longwave irradiance can be estimated from shortwave transmittance and air temperature using the algorithm proposed by Sicart et al. (2006) that modified Brutsaert's clear sky longwave algorithm for cloudy conditions. Sky view factor and terrain or vegetation emission of longwave are also included in the Sicart's model and can be significant in mountains (Plüss & Ohmura, 1997) and forests (Pomeroy et al., 2009). All snowmelt models use an albedo routine that can be selected from amongst seven options, including forcing with observed albedo. The area albedo change routine of Gray and Landine (1987) is often used for its consideration of the effects of initiation of snow-covered area depletion on areal albedo during melt of shallow prairie snowcovers. An alternative module of snow albedo change developed by Verseghy (1991) and adopted by Essery and Etchevers (2004) is based on the age, depth, density and temperature of the snow layer and is favoured for continuous and deep snowcovers. There are three other snow and ice albedo routine options for specialised applications, including using observed albedos as model forcing inputs.

Available melt energy can be converted to a melt rate considering the latent heat of fusion and available latent heat by turbulent transfer can be converted to sublimation considering the latent heat of sublimation. CRHM has several options for melt calculations. One is the Energy Budget Snowmelt Model (EBSM, Gray & Landine, 1988), a daily time-step, processes based, parametric, semi-empirical, single layer snowpack snowmelt model based on snowmelt physics described by Male and Gray (1981). This model is robust, has no parameters to set and is well suited for shallow, cold Canadian Prairie snowpacks or for temperate snowpacks where internal energy changes are small. It has been customized to ice and firn melt by adjusting its albedo routine and assuming glacier ice and firn are isothermal, so all internal energy change goes to icemelt or firnmelt (Pradhananga & Pomeroy, 2022). The more physically based, two layer, energy and mass balance snowmelt model – Snobal (Marks et al., 1998), is used more commonly in CRHM to calculate snow melt processes (DeBeer & Pomeroy, 2017). It can simulate the energy and mass balances of deep cold and isothermal snowpacks over glacier and non-glacier surfaces. The turbulent heat fluxes are obtained using an approach adopted from Brutsaert (1982) by Marks and Dozier (1992). Over glaciers, the turbulent fluxes can be calculated to account for the katabatic wind commonly found in glacier environment following a parametrization developed by Oerlemans and Grisogono (2002) and further tested by Munro (2004). Debris-covered glaciers are prominent features of the world's glacierized mountain regions, with the presence of supraglacial debris modifying both the glacier ablation patterns and its response to climatic forcing (Scherler et al., 2018). The effects of debris on glacier surface melt are well-understood: a thin layer of debris (less than several centimetres), or patchy debris, on the glacier surface enhances melt, while a thick layer of debris insulates the underlying ice and reduces melt (Nicholson & Benn, 2006; Östrem, 1959). A routine by Carenzo et al. (2016) has been included to calculate debris-covered glacier icemelt. CRHM can also calculate temperature index and radiation index melt which allow it to simulate less physically based modeling approaches for the purposes of intra-platform comparisons or model falsifications (e.g., Krogh and Pomeroy 2021).

3.5. Glacier mass balance

CRHM simulates the mass balance of the snow/firn/ice water equivalents for glaciers along with the glacier surface elevation and glacier water and ice flow routing (Pradhananga & Pomeroy, 2022). The change in glacier surface elevation is calculated as a function of snow redistribution and accumulation, snow conversion to firn, firn conversion to ice, and ablation of snow, firn and ice. Firn is snow that has survived at least for one summer melt season (Anderson & Benson, 1963), and its densification and conversion to ice is calculated in three temporal stages adopted from semi-empirical steady-state approaches and deployed in an 11-layer snow-firn-ice system. Many models do not consider firn separately from glacier ice (e.g., Li et al., 2015; Naz et al., 2014; Wheater et al., 2022), however firn has important properties for glacier energetics and hydrology. The albedo of firn is lower than that of snow, but it is higher than that of ice. Meltwater routing is slower in firn than in ice (Hannah & Gurnell, 2001).

3.6. Evapotranspiration

The evaporation module provides several options that allow users to diagnose "actual" evaporation, the water vapour physically transferred to the atmosphere, from soil, plants, and free water surfaces. As a complex physical process, diagnosing reasonable estimates of evaporation requires consideration for key interactions between the balance of available energy, aerodynamic water vapour transfer, and the surface water balance. Earlier module developments included the Granger and Gray (1989) method, which can be applied to unsaturated agricultural surfaces and does not have parameters to set except surface aerodynamic roughness. However, for the purposes of hydrological modelling, previous studies (e.g., Armstrong et al., 2010; Pomeroy et al., 2014) needed to modify existing evaporation parameterisations for water limited (e.g., drought via soil moisture coupling) or energy limited conditions (e.g., wet conditions via introduction of the Penman-Monteith (P-M) method (Monteith, 1965)). Evapotranspiration can be modelled more realistically using the P-M approach applied under a range of dry to wet conditions. Parameterisation of the P-M method follows the algorithm described by Armstrong et al. (2008, 2010). This approach uses a standard aerodynamic resistance and a modified Jarvis-type canopy resistance formula (Verseghy et al., 1993) that applies four environmental stress factors describing stomatal controls under suboptimal conditions for plant growth. For free water surfaces (e.g., wetlands, small lakes, and streams), a standard Priestley-Taylor formulation (Priestley & Taylor, 1972) can be applied to estimate actual evaporation assuming advection-free conditions. For large lakes, a bulk transfer formulation, the Meyer Formula, is available (Krogh et al., 2015). All evaporation methods withdraw moisture from free water surfaces first, then intercepted canopy water (Figure 6), then ponded surface water, and finally stored soil moisture restricted by water availability to conserve the water mass balance.

3.7. Hillslope, soils and groundwater

Hillslope hydrology involves surface and subsurface water redistribution and interactive processes such as infiltration, evapotranspiration, overland, subsurface and groundwater flows, which play critical roles in streamflow generation (Kirkby, 1988). Hillslope hydrology derives the inputs from rainfall and snowmelt at the soil surface, which either infiltrate to recharge the upper soil layer or run off as overland flow (Figure 6). The infiltration process in cold regions comprise frozen and unfrozen soils and is influenced by soil texture, initial soil moisture saturation, initial surface saturation and soil temperature (Freeze & Cherry, 1979; Kane & Stein, 1983; Zhao & Gray, 1999). Soil moisture is withdrawn by evapotranspiration into the atmosphere from the rooting depth, which is controlled by plant types, soil texture and biophysical properties of vegetation (Armstrong et al., 2010). In the unsaturated zone, water moves vertically from the upper soil layer to the lower soil layer via pressure gradients and gravity, and excess water from the lower soil layer percolates vertically to the saturated zone, recharging groundwater. Lateral subsurface flow in the unsaturated zone and lateral groundwater flow in the saturated zone redistributes water based on hydraulic gradients along the hillslope. Both subsurface and groundwater flows are important flow pathways in streamflow generation and are complicated by local heterogeneities in hillslopes (Graham et al., 2010) and hydrogeological characteristics underneath the hillslope (Hayashi, 2020). Surface overland flow generated by infiltration-excess or saturation-excess mechanisms is the other flow pathway in streamflow generation and can be delayed by detention layers such as loose organic material on forest floor (Keith et al., 2010) or temporal snow damming (Fang et al., 2013a,b). In areas with heavy soils and intense agricultural activity, artificial subsurface drainage structures (i.e., tile drainage) also influence subsurface water redistribution processes and affect streamflow generation.

CRHM calculates the overland, subsurface and groundwater flows and simulates the groundwater-surface water interactions using a soil module. The soil module was revised from an original soil moisture balance routine developed by Leavesley et al. (1983) and has been modified by recent studies to account for cold regions processes (Dornes et al., 2008; Fang et al., 2010, 2013; Pomeroy et al., 2016a). The soil module now estimates soil moisture and groundwater storage, depressional storage, subsurface flow in soil layers, groundwater flow and surface overland flow with detention layer configuration. The flow rates are calculated using Darcy's law parameterized using the pedotransfer relationship developed by Brooks and Corey (1964). The soil module interacts with evapotranspiration, infiltration and freeze–thaw algorithm modules to estimate evaporation loss and infiltration and simulate freezing-thawing dynamics on water movement in soil layers. A detailed description of these modules for simulating hillslope hydrology is provided in Fang et al. (2013a,b) and Pomeroy et al. (2016a). A new tile drainage module has been developed to calculate the tile outflow rate from tile drainage networks based on soil moisture. It uses an extended version of Hooghoudt's equation (Hooghoudt, 1940) that accounts for the effect of soil capillary fringe on drainable soil water (Skaggs, 1980). CRHM has some limitations in simulating groundwater-surface interactions and groundwater systems. The assumption of surface tension in pore spaces being dominant over gravity is a limitation when simulating preferential flows in subsurface and groundwater layers where coarse-textured and unconsolidated materials overlaying impeding layers or bedrock. The simple "bucket" conceptualization of the groundwater component is another limitation in simulating groundwater-fed streamflow in first-order alpine basins that are controlled by complex groundwater storage-discharge dynamics (Hayashi, 2020).

3.8. Frozen soils and permafrost

The presence of frozen soils plays a key hydrological role on cold regions hydrology driving the energy and mass fluxes exchange between the ground and the atmosphere. In places with permafrost or seasonally frozen soils, infiltration rates depend not only on soils characteristics and available water but also on the degree of ground thaw and soil's

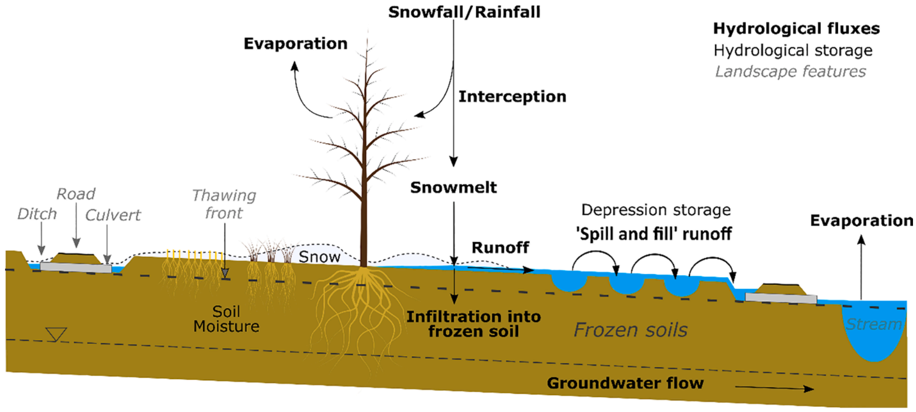

Fig. 7. Conceptualisation of processes governing runoff generation in a Canadian Prairie basin, showing the effect of spill and fill in controlling runoff to streams (Annand, 2022).

water/ice content (Scherler et al., 2010). CRHM includes a set of physically based algorithms to represent processes related to ground freeze and thaw, and infiltration into frozen soils. Infiltration into frozen soil is characterized by two flow regimes: a transient and a quasi-steady-state regime (Zhao et al., 1997). The transient regime occurs immediately after water starts infiltrating where the infiltration rate and heat transfer decrease rapidly as the soil temperature increases through conduction. The quasi-steady-state is characterized by gradual changes in the infiltration rate with time, and soil warming is driven by latent heat released by the refreezing of melted water supplied from upper layers (Zhao et al., 1997). Realistically representing infiltration into frozen soils, and subsurface storage and flow is thus critical to simulate the hydrological regime of cold regions basins (Walvoord & Kurylyk, 2016). Infiltration into frozen soils is represented following Gray et al. (2001), where infiltration is first classified as unlimited, restricted and limited. Infiltration under limited conditions depends on initial surface saturation, average soil saturation and temperature, and infiltration opportunity time and is calculated using a parametric representation of a finite element heat and mass transfer model (Zhao et al., 1997; Zhao & Gray, 1997; 1999) or a simpler model derived from observations in the Canadian Prairies fitted into a physically based framework and forced by the degree of soil saturation and peak snow accumulation before melt (Gray et al., 1986).

CRHM has three different modules options based on XG (2013), Hayashi et al. (2007) and Van Wijk (1963) and more variants to calculate soil freezing fronts. Most algorithms that represent freezing and thawing fronts are based on the Stefan Equation (Juminikis, 1977) that includes heat exchange through conduction and water phase change in homogeneous soils. Modified versions of the Stefan Equation have been implemented to represent multilayered soils (Fox, 1992; Hayashi et al., 2007; Woo et al., 2004; Xie and Gough, 2013). Other solutions to the freezing and thawing front problem that also incorporate advected heat flux have been developed by Lunardini (1998) as shown by Kurylyk et al (2014). Simpler algorithms based on a temperature index have also been included, such as the *n*-factor (Woo et al., 2007). The most preferred options is the XG-Algorithm as it provides an intermediate degree of complexity, fast computation, and allows the calculation of freezing and thawing fronts over multilayered soils (Xie and Gough (2013).

The XG module in CRHM uses a multi-layer, simplified solution of Stefan's Equation (Xie and Gough, 2013) to represent frost table dynamics (freezing and thawing) in partially frozen soils. The XG-algorithm assumes a linear temperature profile in the thawed soil layers to represent heat transfer in multi-layered soils with heterogenous soil properties. XG in CRHM divides the soil into several numerical layers with variable depth to compute the progression of the thawing/freezing front, in which each layer has its own properties (e.g., porosity and thermal conductivity). Ground surface temperature is used as the upper boundary condition, which can be estimated using the radiative-conductive-convection (RCC) method of Williams et al. (2015) or a temperature-index algorithm (Woo et al., 2007) for the snow-free period, and can be estimated using a conduction approach (Luce & Tarboton, 2010) by coupling to the energetics of the Snobal snowpack module for the snow-covered period. As the thawing front advances through the summer, subsurface water storage capacity increases proportionally to the maximum subsurface capacity.

Where there is permafrost, infiltration is restricted by the position of the frost table and the subsurface water storage capacity. Frost table and infiltration into frozen soils are tightly coupled with the snowpack, evapotranspiration, infiltration and soil moisture processes. For example, ground thaw does not start until the snowpack is completely depleted, evapotranspiration cannot access water below the frost table, and the thermal conductivity of the soil layers depend on the soil moisture content, which in turn depends on lateral water redistribution. In permafrost soils, the non-frozen soil layer between the ground surface and the uppermost permafrost layer defines the active layer, which varies spatially (e.g., north- versus south-facing slopes (Carey & Woo, 2005)) and temporally through the season as the air temperature raises after the winter. Ground thaw primarily depends on the energy available to warm the soil and the soil's heat conductivity capacity which, in turn, depends on factors such as water/ice content, porosity, and texture (Ling & Zhang, 2004; Zhao et al., 1997). The depth of the active layer controls the available soil depth capacity for water transport and storage, mediating runoff generation. For example, Quinton and Gray (2001) showed that the hydraulic conductivity of organic soils can decrease several orders of magnitude with depth. Krogh et al. (2017) and Krogh & Pomeroy (2021) describe CRHM's representation of permafrost dynamics and model validation in detail.

3.9. *Depressional storage and variable contributing areas for runoff generation*

Much of the prairies of Western Canada and the northern United States lie within the "Prairie Pothole Region", where the hydrography is dominated by millions of surface depressions known as potholes or "sloughs". These depressions trap surface runoff, which in Canada is predominantly from the spring melt of the accumulated winter snowpack. Because much of the region is underlain by glacial till, which generally has very low hydraulic conductivities, the infiltration of the water is restricted (van der Kamp & Hayashi, 1998). When depressions are filled, additional runoff or direct precipitation will flow overland to neighbouring depressions, the phenomenon being known as "fill and spill" runoff (Spence & Woo, 2003). Fill and spill influenced runoff occurs not only in the Prairies, but in the circumpolar boreal forest, Arctic

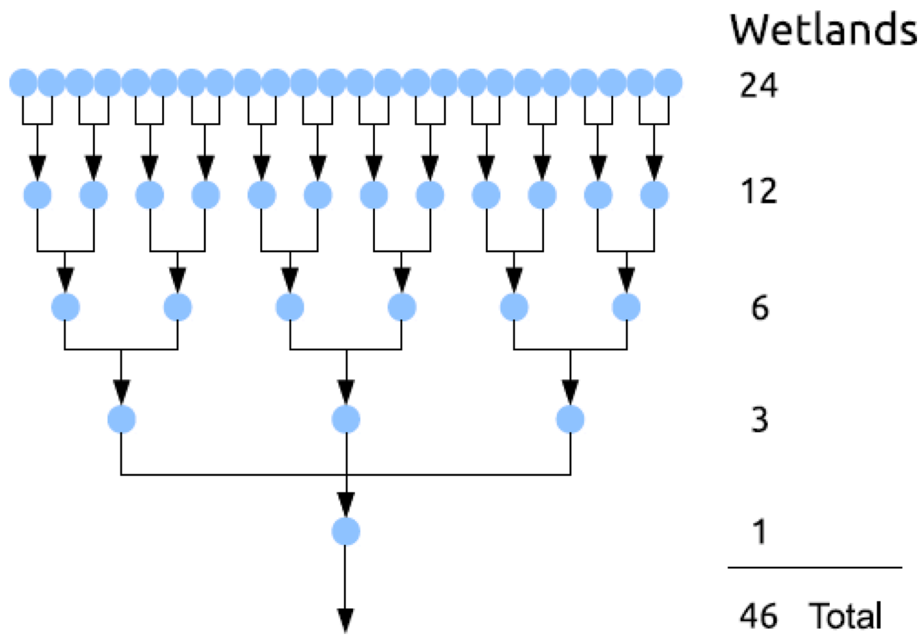

Fig. 8. Schematic diagram of arrangement of dynamical wetland network developed from the Pothole Cascade Model (Shook & Pomeroy, 2011b).

tundra and other wetland and lake-dominated regions with moderate topography, and so is a globally important streamflow generation mechanism.

The trapping and release of fill and spill runoff depends on water storage in the depressions (Fig. 7). Therefore, the fraction of a basin dominated by depressions that can contribute flow to the outlet also varies with surface water storage. When depressions in a basin have available storage capacity, they can retain surface runoff and the area contributing flow to these depressions does not contribute flow to the basin outlet. Conversely, when depressions are filled, then they cannot retain runoff, and their contributing area can contribute flow to the basin outlet. The relationship between the storages of water and the contributing fractions of Prairie basins is nonlinear and hysteretic, due to the very large numbers of state variables (water storages in the depressions) and their complex interactions (Shook et al., 2013, Shook et al., 2021).

Most hydrological models are unable to simulate varying contributing fractions of basins, although several hydraulic models have been developed to address the problem, including the Wetland DEM Ponding Model (Shook et al., 2013) and FLUXOS-OVERLAND (Costa et al., 2020). Unfortunately, these models are computationally expensive and cannot be easily incorporated within hydrological models. The Pothole Cascade Model (PCM, Shook et al., 2013) is an alternative. It is a relatively simple model that simulates fill and spill from depressional storage based on the explicit representation of flow sequences to arrangements of individual depressions (Fig. 8). The model has been shown to produce connected/contributing fractions similar to those of the more complex models (Shook et al., 2013). The PCM has been incorporated in CRHM by using HRUs to simulate networks of connecting depressions (Fig. 8). Although the number of depressions in a given basin is much greater than can be simulated by CRHM, the model is able to compensate by simulating a representative fraction of the depression network with each depression being represented by a HRU with its own runoff contributing area. The outflow from the modelled fraction is then scaled to represent the entire basin. This approach has been applied successfully to several prairie basins (Pomeroy et al., 2012b, 2014).

3.10. Nutrient dynamics

CRHM has been extended to simulate water quality concentrations and fluxes of Nitrogen (N, five species) and Phosphorus (P, five species) based on the research of Roste (2015) and Costa et al. (2017) and based on the water quality process simulations developed in the HYPE model (Lindström et al., 2010), with similar parameterisation needs. This extension is motivated by the recognition that nutrient pollution and eutrophication of major lakes are also major environmental challenges in many cold regions around the world (Smith et al., 2006, 2019).

Cold regions biogeochemistry processes have not been adequately represented by conventional rainfall-runoff models (Costa et al., 2020). N and P transport and transformation processes are challenging to simulate due to the effect of seasonal snow cover (Brooks et al., 1996; Jones, 1987; Mladenov et al., 2012), soil freezing (Brooks et al., 1996; Cade-Menun et al., 2013; Clark et al., 2009; Jones, 1999; Pellerin et al., 2012; Peters & Driscoll, 1987; Sebestyen et al., 2008; Snider et al., 2017), and lake/wetland freeze-up on soil–plant systems, soil biogeochemical cycling, microbial activity, and plant uptake (Cober et al., 2018; Costa et al., 2019; Elliott, 2013; Liu et al., 2013, 2019; White, 1973). Soil management and agricultural practices, such as fertilizer use, tillage practices (Miller et al., 1994; Timmons et al., 1970; Ulén, 1997) and wetland drainage, further hinder the application and effectiveness of existing nutrient models (Baulch et al., 2019; Costa et al., 2020; Irvine et al., 2019; Van Esbroeck et al., 2017). Models that rely excessively on tuned and lumped parameters are prone to fail to capture the nuances of these processes, making them less reliable for future climate projections and non-stationary scenarios.

CRHM integrates hydro-biogeochemical drivers at agricultural field and sub-basin scales. For example, agricultural activities can be explicitly represented in the model, such as fertilizer/manure application that can strongly impact the amount of soil nutrients mobilized with runoff. Other sources such as atmospheric deposition and plant residue, as well as sinks like plant uptake, can also be considered. Chemical transformations calculated include mineralization (for N and P), nitrification (N), denitrification (N), degradation (N and P), dissolution (N and P) and dynamic sorption–desorption equilibrium (P) with sediments. Transformation rates are computed dynamically by modulating reference values (determined at 20 °C) to changes in soil temperature and moisture. The ability to capture spatio-temporal hydro-biogeochemical variations at high temporal resolution during snowmelt via energy-budget calculations (hourly and sub-hourly) makes the model exceptionally suited for capturing both streamflow and nutrient export during the

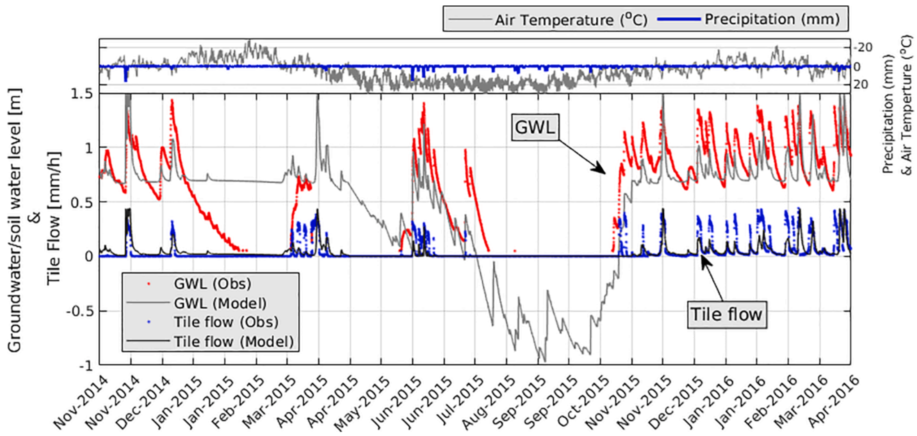

Fig. 9. Comparison between observed and simulated tile flow, observed and simulated groundwater/soil water level (GWL), and observed air temperature and precipitation in a farm field in the Lake Erie Basin, southern Ontario, Canada (43° 38′ 24″ N, 81° 24′ 44″ W).

short but critical snowmelt period (Baulch et al., 2019; Costa et al., 2017; Kokulan et al., 2019). The modelling of nutrient transport phenomena is integrated within many core modules and extends to the runoff and routing calculations in CRHM.

3.11. *Streamflow synthesis*

Streamflow synthesis requires simulations of hydrological processes and calculations of flux and state variables in the hydrology cycle to estimate surface runoff, subsurface flow, groundwater flow and channel precipitation that are the main sources of streamflow for a drainage basin. Predicting streamflow at the basin outlet involves the routing of surface runoff, subsurface flow and groundwater flow as well as channel routing, which considers the effects of storage and dynamics of a system such as land surface, depression ponds, soil layers, groundwater or channel on the shape and movement of various flow hydrographs. Routing can be classified by different criteria: (1) lumped flow or distributed flow routing based on spatial and temporal variations, (2) hydrological or hydraulic routing based on governing equations, and (3) river flow, reservoir, or overland flow routing based on watercourse type. Streamflow synthesis is one of the most important aspects in hydrology for flood forecasting, reservoir operation and water resource management, but it is highly challenging in cold regions because of the strong seasonal dynamics of frozen soil and snow storage.

For HRU routing in a basin, CRHM can use Clark's lag and route algorithm based on time-area unit hydrograph theory (Clark, 1945) for subsurface and groundwater flows, and Clark's algorithm or Muskingum method based on a variable discharge-storage relationship (Chow, 1964) for surface runoff. Routing sequence can be from one HRU to another HRU for Clark's algorithm or from one HRU to multiple HRUs for Muskingum method, with a modified Hack's law to estimate routing lengths from HRU areas (Fang et al., 2010) and to allocate amount of routed flow between HRUs based on their relative lengths. Manning's equation is used to estimate the mean flow velocity in the channel, with parameters calculated from the channel condition and the gradient of the drainage network. For large river basins, CRHM uses "representative basin" (RB) groups to simulate hydrological processes for sub-basins and uses a Muskingum routing group to connect and route the sub-basin streamflow to the outlet of the river basin. Details of parameterization and setup for CRHM streamflow routing are provided in recent studies (Fang et al., 2010, 2013; Pomeroy et al., 2013, Pomeroy et al., 2014). Routing methods in CRHM do not incorporate ice jam and backwater into river flow routing and mainly estimate the natural flow without reservoir operations, which are some limitations of CRHM in streamflow simulation for large and low relief river basins in cold regions. However, routing on glaciers is considered in that melt from ice and firn melt is routed through linear reservoirs before being released to the soil routine.

4. Research basin hydrological process diagnosis

CRHM has a unique capability to integrate with field investigations in research basins to demonstrate the impacts of improved process descriptions on hydrological prediction and to constrain calculations of hydrological processes from the results of process studies in the basin. As it is a modelling platform for scientists, it can be changed and developed sequentially to reflect hydrological discoveries and advances in research basins. Its emphasis on permitting model failure rather than parameter calibration makes the importance of advances in understanding very clear in model outputs. Model performance metrics against multiple prediction objectives ranging from snow and glaciers, to evapotranspiration, soil moisture, and groundwater, to streamflow discharge and water chemistry are shown in the Appendix, Table 1. The following examples show CRHM's application in agricultural, forest, permafrost and high mountain basins in cold and temperate regions to diagnose specific aspects of how agricultural drainage, tillage and fertilizer application, permafrost and glaciation impact snowpacks, soil moisture, groundwater, streamflow, and hydrochemistry.

4.1. *Impacts of tile drainage on agricultural runoff*

Artificial tile drainage is an essential agricultural management practice in many regions around the world, including in cold climates. However, recent studies suggest that these systems may exacerbate the effect of climate change in increasing nutrient export (Haghnazari et al., 2020). Tile drainage systems drain about 14 % of farmlands in Canada (ICID, 2018; Kokulan et al., 2019). In southern Ontario, Canada, tile drainage is present in 45 % of the fields, especially in the southwestern part where fine-grained and clay soils pose challenges for water management (Plach et al., 2018; Van Esbroeck et al., 2016).

Many agricultural lands in southern Ontario with tile drainage systems have shallow soil layers separated from the deeper groundwater system by an impermeable or semi-impermeable layer (Broughton & Jutras, 2013). These layers with low hydraulic conductivity prevent the free drainage of water from shallow to deeper soil and groundwater systems. Snowmelt, partially frozen soils and freeze–thaw events due to large temperature variations in the cold season further contribute to the ponding of water in surface depressions and the need for tile drainage (Lam et al., 2016; Macrae et al., 2007, Macrae et al., 2019). During large temperature oscillations, heavy rainfall and surface ponding are common, and the thick capillary fringe that develops in the fine-grained (clay and clay-loam) soils compromises its natural drainage capacity.

The tile drainage module developed for CRHM enables simulation of

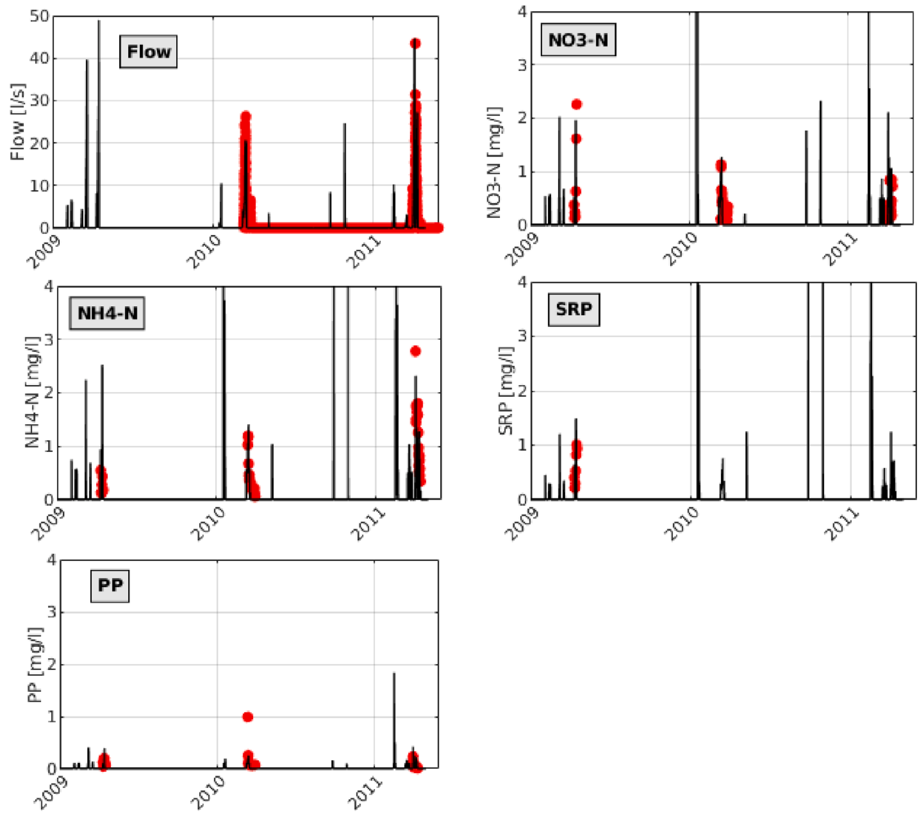

Fig. 10. Comparison between observed (red dots) and simulated discharge (black lines) of water (Flow), NO_3, NH_4-N, SRP and PP at South Tobacco Creek, Manitoba, Canada. (For interpretation of the references to colour in this figure legend, the reader is referred to the web version of this article.)

these cold agricultural regions and evaluation of management options (Kompanizare et al., 2022). Tile flow is calculated based on a modified version of the Hooghoudt (1940) equation that accounts for capillary fringe development, which causes the saturation of soil above the water table and reduces soil drainable water (Skaggs, 1980). Fig. 9 shows the results obtained for an application to a farm field in southern Ontario. The model was able to capture the flashy response of the tiles and their effect on the seasonal groundwater table. Results showed that tile flow was able to rapidly reduce soil moisture and lateral overland flow to adjacent fields. The groundwater table oscillated drastically between seasons, influencing the tile flow response. In the growing season, low precipitation and higher evapotranspiration rates often caused minimal tile flows. This analysis informs evaluations of tile drainage impacts on Lake Erie hydrology and water quality.

4.2. Nutrient export from agricultural basins

The CRHM water quality modules derived from HYPE have been used to investigate the dynamics of nitrogen (N) and phosphorus (P) in a small basin that contributes to the flow of the Red River into Lake Winnipeg, Manitoba, Canada. Lake Winnipeg is the 10th largest in the world and, similarly to other lakes in North America such as Lake Erie, has been increasingly threatened by enhanced aquatic productivity and the occurrence of algal (Schindler et al., 2012) due to excessive nutrient load. The small basin examined in this study is the Steppler Basin (SB), which is located in the headwaters of the South Tobacco Creek Basin (STCB). SB is a 205-ha agricultural basin comprising 42 farm fields that are used to grow cereal grains and oilseeds on a rotating basis, as well as a beef cattle herd. Beneficial Management Practices (BMPs) were initiated in 2005 and include a holding pond, riparian zone, grassed waterway, grazing restrictions, forage conversion, and nutrient management.

The model was set up to explicitly simulate the 42 individual farm fields in SB. Meteorological observations were used to force the model hydrology, whilst fertilizer, manure and plant residue loading information, as well as tillage practices, were used to force and parameterise the HYPE water quality modules in CRHM. Model predictions were evaluated against observations at 5 locations in the basin between 2005 and 2011. This included (1) snow water equivalent (SWE) and (2) streamflow for hydrological model validation and (3) two nitrogen species (nitrate, NO_3; and ammonium, NH_4) and (4) two phosphorus species (soluble reactive phosphorus, SRP; and particulate phosphorous, PP) for biogeochemical model validation. Costa et al. (2017), Liu et al. (2014) and Mahmood et al. (2017) provide details on model setup in this basin.

Fig. 10 compares observations and simulations for both hydrological and water quality variables. The flashy spring freshet accounted for 21 % of the annual streamflow and 30 %, 31 %, 20 % and 16 % of the annual NO_3, NH_4, SRP and PP export load on average. The results highlighted the importance of parameterising a water quality model with the amount, type, placement and timing of fertilizer and manure application, as these have strong controls on nutrient export (e.g., Duncan et al., 2017; Grant et al., 2019; Plach et al., 2018). Tillage practices (i.e., broadcast, incorporated, with seeding) affect the depth at which nutrient inputs were placed in the soil and also influence nutrient availability to runoff transport. The model, parameterised with these practices, simulated the extremely flashy and episodic discharges of these nutrients during snowmelt freshet. This shows the importance of snow and frozen ground hydrological processes along with nutrient dynamics and land use practices in simulating water quality dynamics in cold climate agricultural basins. By demonstrating that the CRHM with suitable water quality process simulations, can predict chemical transport that results from agricultural land management, a concrete, transformative direction for innovation in basin nutrient modelling in Canada and other cold regions is outlined. Appropriate cold regions hydrological models are needed to provide advanced background hydrology to

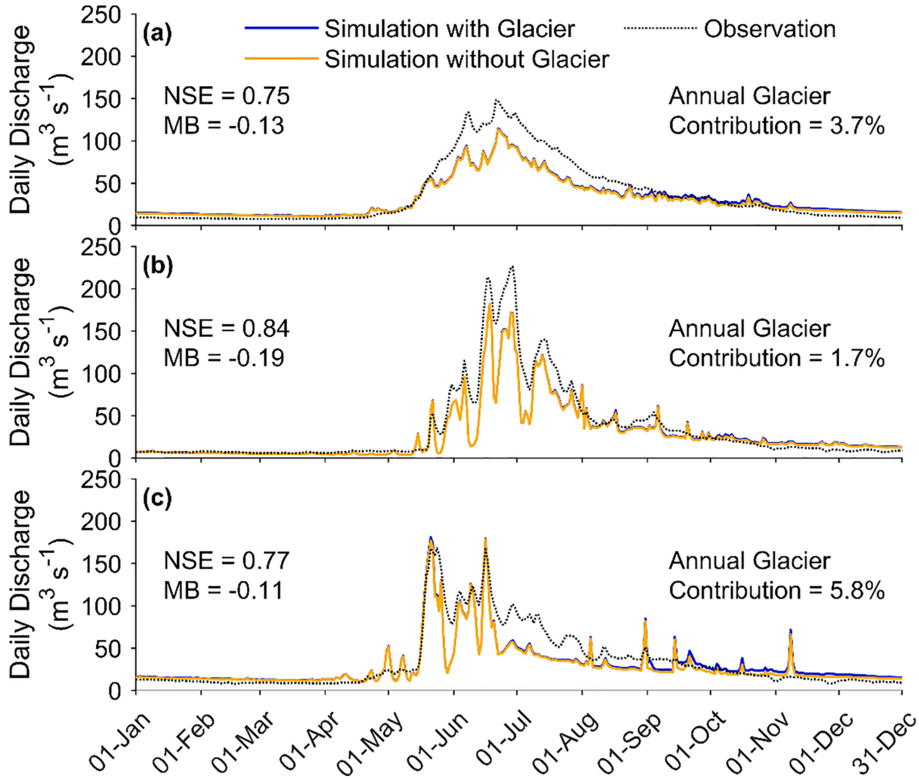

Fig. 11. Comparison of the simulated mean annual daily discharge with and without glacier for the Bow River at Banff for (a) 2000–2015, (b) cold year (2002) and (c) warm year (2006). The observation is the daily streamflow observed at Water Survey of Canada gauge 05BB001 (Banff, Alberta, Canada).

support comprehensive water quality dynamics simulations.

4.3. Diagnosing glacier contributions to mountain streamflow

The Bow River at Banff basin (BRB, 2192 km^2) originates in the eastern slopes of the Canadian Rockies and forms a principal headwater of the South Saskatchewan River in Alberta, Canada. The basin has experienced glacier retreat since the early 20th Century and glaciers covered approximately 1.7 % of the BRB in 2005 (Bolch et al., 2010). Glacier coverage is projected to be minimal by the end of the 21st Century (Clarke et al., 2015). To investigate recent glacier contributions to streamflow in the BRB in order to determine what the losses of streamflow might be in a deglaciated future, a CRHM model was constructed to simulate relevant snow, ice and rainfall runoff streamflow generation processes for high mountains, such as blowing snow, avalanching snow, snow interception and sublimation, energy budget snow and glacier melt, infiltration to frozen and unfrozen soils, hillslope water redistribution, lake water storage and evaporation, evapotranspiration, groundwater flow, surface and sub-surface runoff and open channel flow. The hydrological model was entirely parameterised from local research results and observable quantities, instead of relying on calibration. A high-resolution weather model, a regional run at 4-km resolution of the Weather Research and Forecasting (WRF) model (Li et al., 2019) bounded by ERA-Interim outputs, provided forcing near-surface meteorological variables during 2000–2015. A detailed description of the hydrological model setup is provided in Fang and Pomeroy, n.d. . Two model simulations were conducted for the BRB, “with glacier” (2005 coverage, Bolch et al., 2010) and “without glacier” (minimal coverage expected for the end of the 21st C, Clarke et al., 2015). The model simulation with glacier was evaluated against observed streamflow (Water Survey of Canada gauge 05BB001), and the proportional change in the streamflow as result of glacier melt (sum of firn and ice melt) between the two simulations was used to estimate the glacier contribution to streamflow for the 15-year mean (2000–2015), cold (2002) and warm (2006) years.

The uncalibrated model provided good predictions of daily streamflow for the BRB (Fig. 11), with Nash–Sutcliffe efficiency (NSE) (Nash & Sutcliffe, 1970) values of 0.75, 0.84 and 0.77 and model bias (MB) (Fang et al., 2013a,b) values of −0.13, −0.19 and −0.11 for the 15-year, 2002 and 2006, respectively. The 15-year mean annual glacier contribution to streamflow in the BRB was 3.7 % (Fig. 11a), while glacier melt accounted for 1.7 % and 5.8 % of annual streamflow in the cold (2002, Fig. 11b) and warm (2006, Fig. 11c) years, respectively. The mean annual glacier contribution to streamflow for Bow River at Banff during 2000–2015 was lower than the 4.9 % mean annual glacier contribution during 2000–2009 estimated by Bash and Marshall (2014) but higher than the mean annual contribution values of 1.98 % estimated for 1952–1993 by Hopkinson and Young (1998), the 2.2 % for 1975–1998 estimated by Comeau et al. (2009) or the 2.8 % for 1976–1998 estimated by Demuth et al. (2008). These differences likely result from interannual variabilities of streamflow and glacier wastage during these different periods as well as differing estimation methodologies and available forcing data.

4.4. Arctic droughts and floods

Arctic hydrology has many challenges for hydrological diagnosis and prediction. This remote region is sparsely gauged with few long-term research basin (Laudon et al., 2017) which restricts the opportunity to use observations to diagnose hydrological change and to inform the development of hydrological models. The Arctic supports a wide range of complex biophysical processes (Bring et al., 2016), including the presence of permafrost and/or seasonally frozen ground, controlling subsurface and surface mass and energy fluxes through thermodynamics. These characteristics make northern regions a particularly challenging environment for hydrological models; yet hydrological and permafrost thaw predictions are needed to design infrastructure, to manage water and to evaluate ecosystem services (Bring et al., 2016;

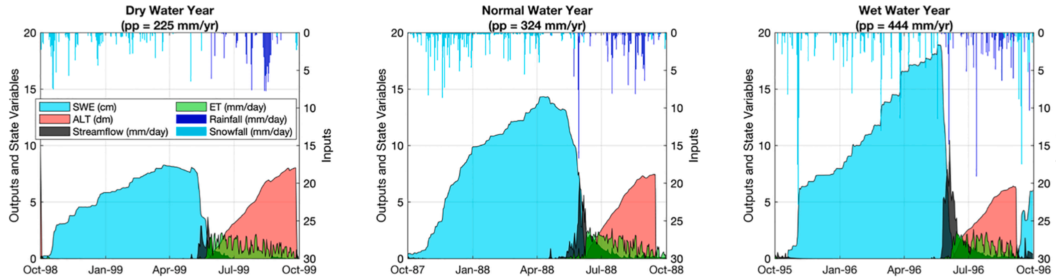

Fig. 12. Snow, evapotranspiration, precipitation, streamflow and active layer thickness over permafrost in Havikpak Creek Basin, Northwest Territories, Canada. Panels show a selection of three water years (October-September) under dry, normal and wet conditions. Note the different units used for outputs (streamflow and evapotranspiration (ET) in mm/day) and state variables (snow water equivalent (SWE; cm) and active layer thickness (ALT, dm)) for better comparison. Data from simulations by Krogh et al. (2017).

Hjort et al., 2018; Lique et al., 2016; Schuur et al., 2015).

A small permafrost-underlain, Arctic basin near Inuvik, Northwest Territories, Canada (16.4 km^2, Havikpak Creek) was simulated using CRHM (Krogh et al., 2017) to evaluate the contribution of differing hydrological processes to the water balance and streamflow generation using the CRHM platform. This model configuration incorporates key Arctic hydrological processes including snowpack energy balance, blowing snow redistribution and sublimation, canopy interception, ground freeze and thaw, infiltration into frozen and unfrozen soils, evapotranspiration, surface and subsurface flow and storage, and streamflow routing. The permafrost representation, see Frozen Soils and Permafrost section, is a novel treatment of the ground freeze and thaw algorithm and its interaction with other physical processes.

Three water years (dry, normal and wet) were selected to highlight the interactions between key physical processes at the basin scale (Fig. 12). The example shows the impact of a deeper, longer-lasting snowpack on the development of the permafrost active layer thickness (ALT). In a dry year, with a relatively low 8 cm peak SWE, the snowpack fully ablated by the end of May allowing an earlier initiation of ground thaw (red area, Fig. 12) that resulted in an 80 cm deep ALT by the end of the summer. In contrast, in a wetter year with a much deeper snowpack (180 mm peak SWE) that fully ablated by June 23 (about three weeks later), ground thaw initiation was substantially delayed, resulting in a shallower end-of-the-summer ALT at 64 cm. The latter was also influenced by an earlier accumulation of next-season snow due to the colder and wetter conditions. It is important that such hydrological interactions are properly captured by hydrological models applied to permafrost regions as they impact runoff generation processes, and CRHM has been shown to adequately represent, with little to no calibration, most Arctic hydrological processes (Krogh et al., 2017; Krogh & Pomeroy, 2021).

5. Diagnosis of land use and climate changes

CRHM has easy to manipulate parameters that describe land use boundary conditions and also allow systematic changes to forcing meteorology to examine hydrological sensitivity to climate change. This provides a useful capability to assess the sensitivity of hydrological processes and basin hydrology to change. A few examples of this capability are provided here in diagnoses of the impacts of wetland drainage, forest disturbance and climate change on hydrological processes and streamflow generation from local to global scales.

5.1. *Prairie wetland drainage impact on streamflow volume*

Canadian Prairie wetlands exist in surface depressions that receive blowing snow transport in the winter causing deep snow accumulations that melt and fill the depressions in spring. The impact of depressional storage change on the hydrology of small Canadian Prairie basins has been unclear because of conflicting conclusions on the degree of impact between studies of runoff in very small-scale drainage systems and those of multi-year streamflow characteristics of larger basins and because of the compounding effects of climate change (Dumanski et al., 2015). To better understand and predict the impact of wetland drainage on prairie streams due to breaching of depressions (resulting in lower elevation outlets), CRHM was used to create a model that simulates blowing snow redistribution, snowmelt, infiltration to frozen soils, and the fill and spill of networks of depressions at multiple scales (Pomeroy et al., 2014). This CRHM model was used to simulate the hydrology of Smith Creek Research Basin, Saskatchewan (~400 km^2) with various drainage scenarios. Smith Creek Research Basin has undergone substantial wetland drainage from 1958 when it contained 96 km^2 of depressions (24 % of

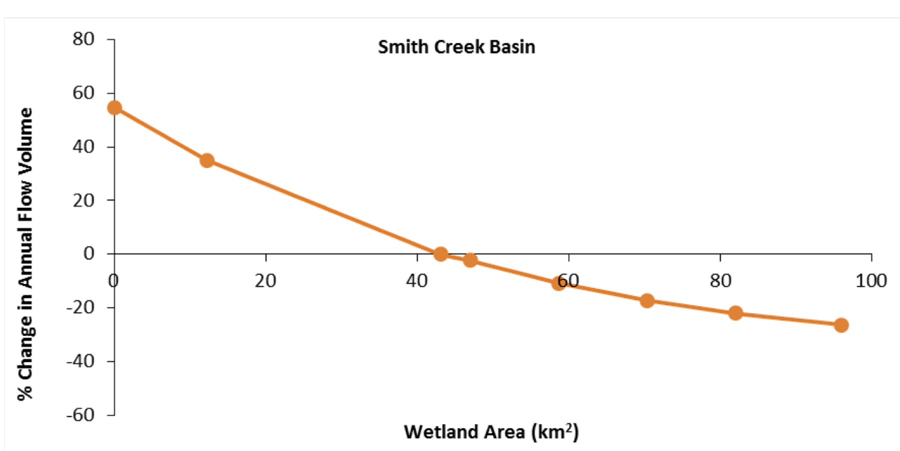

Fig. 13. Fractional change in cumulative annual flow volume over six years with wetland area for Smith Creek Research Basin, Saskatchewan, Canada (Pomeroy et al., 2014).

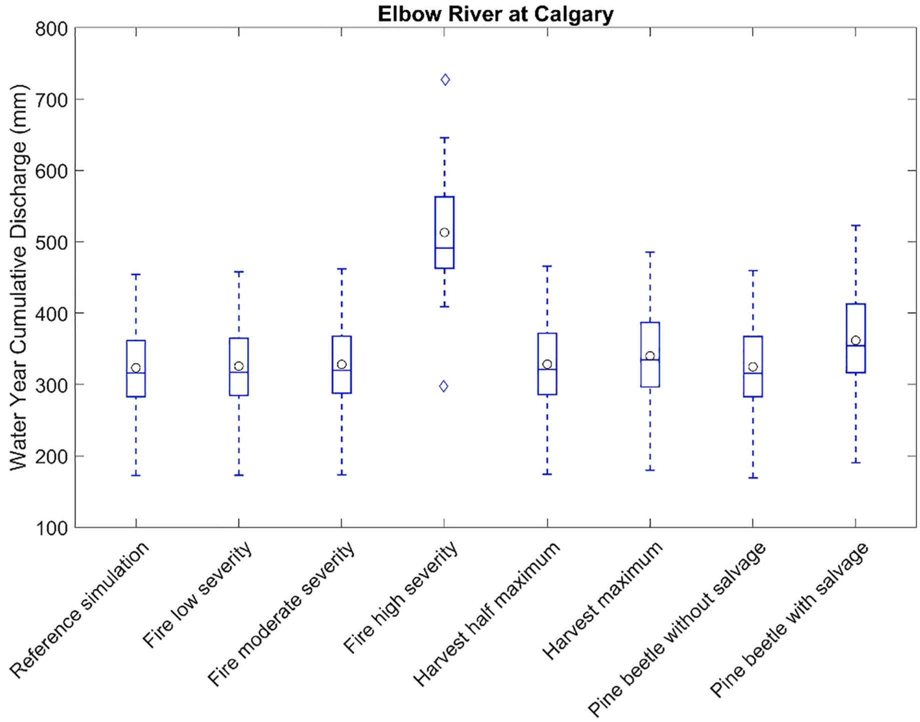

Fig. 14. The simulated annual total discharge for the Elbow River at Calgary, Alberta, Canada for 15 water years. Horizontal line within the box = median value, box = interquartile range (IQR = Q1: 25 % to Q3: 75 %), whiskers = Q1 – 1.5 times the IQR and Q3 + 1.5 times the IQR, diamonds = outliers beyond 1.5 times the IQR, circle = mean value of the 15-water year data.

the basin area) to 43 km^2 (11 % of the basin) in 2008 (Dumanski et al., 2015). CRHM simulations showed that wetland drainage can increase annual and peak daily flows substantially, and that notable increases to estimates of the annual volume and peak daily flow of the flood of record (2011) have derived from drainage to date and will proceed with further wetland drainage. Restoration of depressional storage from the current extent back to that of 1958 decreased the simulated 2011 flood peak by 32 % and the 2011 yearly volume of streamflow by 29 %. Whilst the greatest proportional impacts on the peak daily flows are for dry years, substantial impacts on the peak daily discharge of record (2011) from drainage (+78 %) or restoration (–32 %) are notable and important in Smith Creek and downstream.

The relative response of total basin flow volume over six hydrological years of simulation (2007–2013) shows a non-linear flow response to wetland area change in Fig. 13. This is a useful metric when assessing the effects of wetland change in Smith Creek on water supply for large lakes downstream in Manitoba that have experienced repeated flooding. Drainage-induced decreases in wetland area by 43 km^2 increased the annual flow volume by 55 %, whilst restoration-induced increases in wetland area by 53 km^2 decreased the annual flow volume by 26 %. Smith Creek is already heavily drained, but its flow volumes can still be strongly impacted by further drainage.

5.2. Mountain forest cover change impact on streamflow

The impacts of forest disturbances on streamflow entering Calgary, Alberta, Canada were investigated using a CRHM model of the montane, forested Elbow River Basin (1192 km^2) above Calgary. The model was parameterized from local research results and represent the relevant streamflow generation processes: wind redistribution of snow, gravitational snow transport on steep mountain slopes, glacier accumulation and melt, intercepted snow from forest canopies, infiltration to frozen and unfrozen soils, hillslope sub-surface water redistribution, and evapotranspiration from forests, grassland, clearings and alpine tundra. Bias-corrected near-surface outputs from the Weather Research and Forecasting (WRF) model, bounded by ERA-Interim reanalysis, during October 2000-September 2015 forced the model. Air temperature, vapour pressure, wind speed, incoming shortwave radiation, and precipitation outputs from the 4-km WRF (Li et al., 2019) were bias-corrected using the same outputs from 10-km Global Environmental Multiscale and Canadian Precipitation Analysis (*GEM*-CaPA) produced by Environment and Climate Change Canada, generating an initial 10-km bias-corrected forcing field. Additional precipitation bias correction was performed by a double-mass curve analysis of streamflow from the model runs using the initial 10-km bias corrected WRF and Water Survey of Canada (WSC) streamflow observations from the Elbow River above Calgary.

The hypotheses to be tested were that disturbance of montane forests by wildfire, pine beetle kill and harvesting will increase streamflow volumes and peak flows by reducing evapotranspiration and sublimation from the forest canopy and reducing infiltration to soils through compaction (harvesting), hydrophobicity (wildfire) or increased saturation from reduced root withdrawals for evapotranspiration (all). Simulations of forest disturbances were conducted to examine the hydrological sensitivity to disturbance for three types of scenarios: wildfire affecting all forests, mountain pine beetle (*Dendroctonus ponderosae Hopkins)* infestation of lodgepole pine (*Pinus contorta* var. *latifolia*) forests, salvage harvesting of beetle-killed lodgepole pine forests and harvesting of all pine forests. Forest canopy parameters and soil parameters for infiltration were adjusted for three wildfire severity scenarios, ranging from a 20 % reduction in forest canopy leaf area for low wildfire severity to an 80 % reduction in forest canopy leaf area with development of hydrophobic soils of lower infiltration capacity for the high wildfire severity scenario. Two lodgepole pine forest harvesting scenarios were created: half of the maximum harvest area (25 % pine area) and the maximum harvest area (50 % pine area), by adjusting the lodgepole pine forest area, forest canopy leaf area and soil storage capacity parameters to reflect the impacts of tree removal and soil compaction from harvesting activities. Two scenarios for the final stage of mountain pine beetle infestation were set up, for both scenarios the

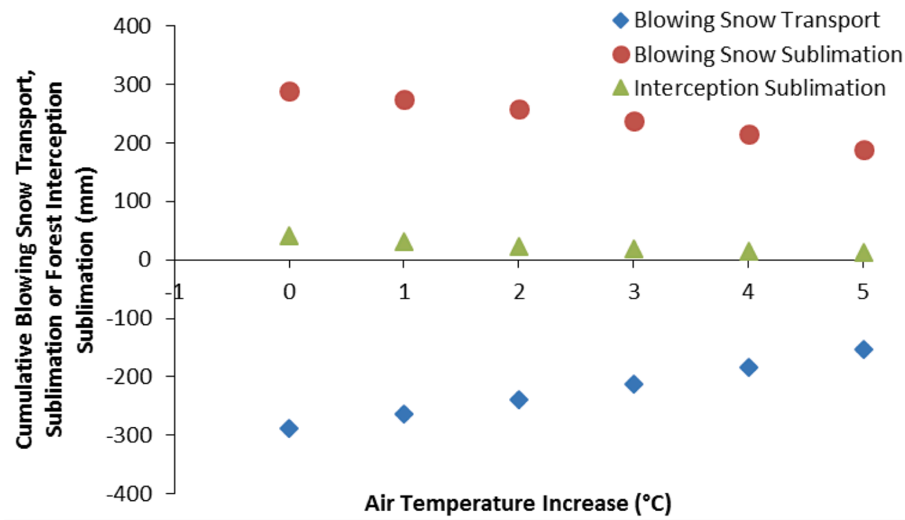

Fig. 15. Snow redistribution and sublimation fluxes at MCRB with warming. Blowing snow transport and sublimation in the alpine are shown as negative and positive respectively when a mass loss to snowpack. Intercepted snow sublimation in the forest is shown as positive when a mass loss from the snowpack. (Pomeroy et al., 2015).

entire lodgepole pine forest was impacted by beetle-kill, with one allowing salvage-logging and harvesting-related impacts on soils as well as canopy, and the other retaining the standing, dead lodgepole pine trees and leaving soil storage parameters undisturbed. The hydrological impacts of forest disturbance focussed on three main changes to hydrological processes in CRHM that set up conditions in which to test the three hypotheses. These process changes resulted from model parameters changed to reflect the different forest disturbance scenarios: i) reduced interception losses of rainfall and snowfall, ii) faster snowmelt and lower evapotranspiration, iii) reduced soil moisture storage capacity due to reduced infiltration, wetter soils and/or soil compaction.

The results (Fig. 14) show strong streamflow sensitivity to extreme wildfire and modest sensitivity to the impacts of mountain pine beetle followed by salvage logging and a weak sensitivity to forest harvesting. The mean annual flow volume over 15-water years for the high wildfire severity scenario increased from 324 mm to 513 mm – a 59 % increase, for the lodgepole pine mountain beetle infestation with salvage logging scenario it increased to 362 mm – an 11 % increase and for the maximum forest harvest scenario it increased to 340 mm, a 5 % increase. Impacts of other forest disturbance scenarios were minor and within 1.5 %.

The simulations were also instructive in examining sensitivity to the recent flood of record – the June 2013 flood (Pomeroy et al., 2016b) where the reference simulation estimated an event flow volume of 70,140 dam^3. High wildfire severity produced the greatest increase in total flow volume to 109,123 dam^3, a 56 % increase. The total flow volume increased to 85,152 dam^3 (21 % increase), 90,763 dam^3 (29 % increase) for harvest at half maximum and harvest maximum scenarios, respectively. For mountain pine beetle scenarios, the increase in the total flow volume during flood was higher with salvage (101,736 dam^3 or 45 % increase) compared to without salvage logging (80,012 dam^3 or 14 % increase). These results show a strong sensitivity of flood peak volumes to land use in this basin – something of concern for the downstream communities.

5.3. Climate change impacts on mountain snowpacks

Climate change is expected to alter Canadian Rockies hydrology substantially because of the importance of snowmelt to streamflow generation (Pomeroy et al., 2012; Fang et al., 2013a,b) and the impact of warming on temperature-sensitive snow processes (Woo & Pomeroy, 2012; Zhang et al., 2000). The Canadian Rockies region has experienced substantial climate warming and low elevation snowpack decline and is anticipated to undergo further warming due to anthropogenic climate change (Clarke et al., 2015; Harder et al., 2015; Pradhananga & Pomeroy, 2022). To better understand the sensitivity of snow processes to warming, Pomeroy et al. (2015) built a spatially detailed physically based snow hydrology model for Marmot Creek Research Basin (MCRB), Alberta, Canada (Fig. 1) using the CRHM platform and used the model to assess the snow hydrology of a high elevation alpine tundra environment (2325 m.a.s.l.) and two medium elevation environments (1845 m a.s.l.), one densely forested (spruce, fir) and the other a small forest clearing (~100 m diameter). Processes modelled included calculation of precipitation phase, snow redistribution by wind, snow interception and canopy unloading, sublimation from blowing, intercepted and surface snow, and energy budget snowmelt. The model was forced with current meteorology from station observations, high quality hourly measurements over nine years (2005–2014), and then with perturbed climates with increased temperature, holding relative humidity constant (allowing vapour pressure to increase) based on the delta method.

Increasing temperatures increased the rainfall fraction of precipitation which reduced snow water equivalent (SWE), but also limited blowing snow erodibility. Warming also enhanced unloading of snow

Table 1
Change in snowfall, peak SWE, blowing snow transport, intercepted snow sublimation, melt rate and snow free date per degree of warming for alpine, forest and clearing environments in MCRB compared to the current climate. Rates shown are averaged over 5 °C of warming.

	Snowfall mm/°C	Peak SWE mm/ °C	Blowing Snow Transport mm/ °C	Blowing Snow Sublimation mm/ °C	Intercepted Snow Sublimation mm/ °C	Melt Rate mm/ (°C day)	Snow Free Date day/ °C
Alpine	−8.3	−11	−9.4	−7.0	n/a	−10.8	−6.4
Forest	−11	−18.6	n/a	n/a	−14.3	−18.7	−7.4
Clearing	−10.9	−17.3	n/a	n/a	n/a	−17.6	−5.5

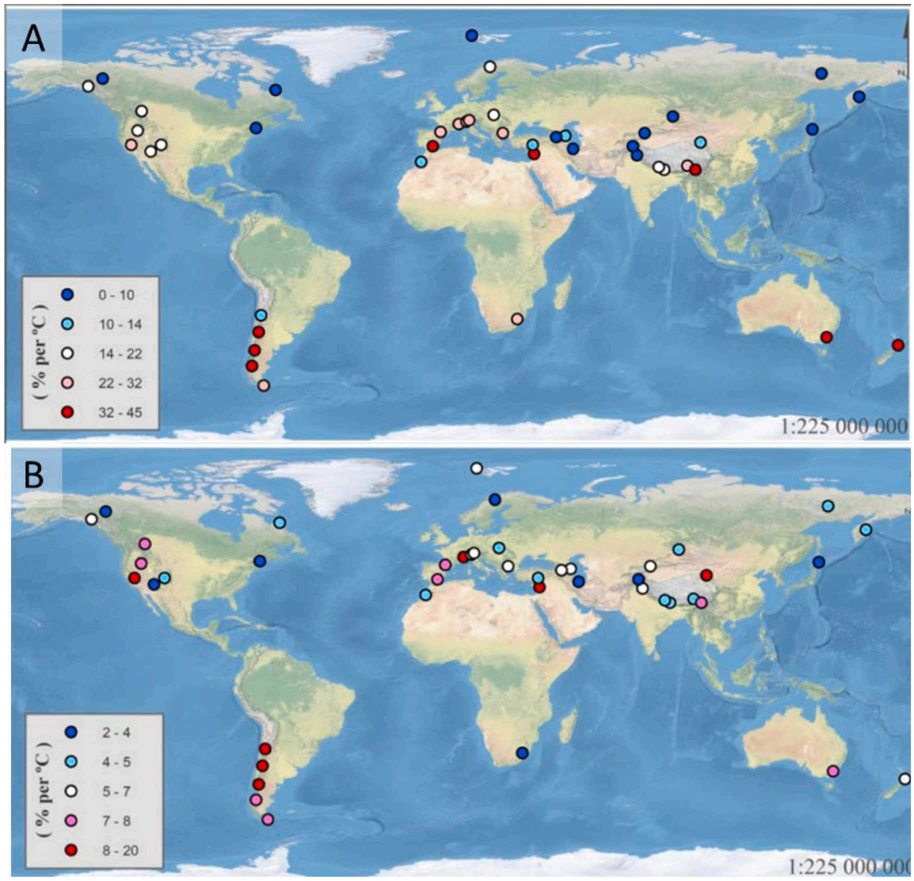

Fig. 16. Sensitivity (decrease in % change per °C of warming) of mean annual peak snow water equivalent (A) and the annual snowmelt rate (B) (López-Moreno et al., 2020).

from conifers which reduced sublimation losses and so increased peak SWE. Increasing temperatures accelerated the initiation of snow ablation by increasing incoming longwave, turbulent and advected heat fluxes, and reducing albedo, but advanced ablation into periods of lower insolation that sustained slower snowmelt. Whilst snowfall in the alpine was proportionately reduced more than the lower elevation sites, peak SWE was most reduced in the forest and then the clearing. Blowing snow ablation processes (transport and sublimation) common in the alpine were reduced more than intercepted snow ablation (sublimation) processes found in the forest (Fig. 15). As shown in Table 1, melt rate reductions with warming were greatest under forest canopies followed by clearings, with much smaller reductions found for the high elevation alpine environment. This is likely due to the advance of mid-summer melting from June and July closer to the solstice period of peak insolation, rather than further away as occurred at the lower elevation sites where snow melts in April and May. The advance of the snow-free date was longest in the forest, followed by the alpine and then the clearing environments. Impacts did not proceed linearly with rising temperatures; 2 °C of warming led to a shift from snowfall to rainfall dominance, a substantial decline in snowpacks and shortening of snow seasons at all elevations. However, 5 °C of warming led to ephemeral low elevation forest snowpacks and an order of magnitude reduction in high elevations snowpacks, with snow-free dates advancing by from four to six weeks.

5.4. Global assessment of alpine climate change impacts on snow hydrology

The high versatility of CRHM for application under contrasting climatic and environmental conditions enables assessment of how snow and hydrological regimes will respond and interact under climate warming (López-Moreno et al., 2020). Thus, an idealized virtual alpine basin was synthesized in CRHM and simulated for 44 mountainous areas around the world, using available long-term bias-corrected global gridded climatic datasets (Weedon et al., 2014). The results showed that snowpacks worldwide will be reduced by climate warming, and a generalized decoupling of mountain river hydrology from snowpack regimes is foreseen in many alpine areas. However, the study also revealed much complexity behind this generalization because snow and hydrological regimes under the different climatic conditions will respond with differing sensitivity to the same levels of warming (Fig. 16). The variability of the sensitivity of rainfall ratio and peak snow water equivalent (SWE) to warming were closely related to the joint effect of air temperature and humidity. However, the sensitivity of snowcover duration to warming was more difficult to characterise because of the more complex processes affecting the response of snow accumulation, redistribution and melt to changing temperatures (e.g., radiative fluxes, wind redistribution and sublimation). The sensitivity of snowmelt rate and peak SWE to warming were closely related; but melt rate sensitivity was substantially lower, decreasing mostly between 5 % and 10 % per °C, than peak SWE sensitivity, which decreased mostly between 10 % and 30 % per °C. This is because of the proximity of the melt period to the summer solstice; warming only slows melt rates when it shifts the melt period into a lower insolation period, and this is not the case for some high alpine snow which after solstice and when shifted can melt closer to solstice. In a further study, López-Moreno et al. (2021) used the same modelling approach to conclude that 75 % of the same alpine basins will undergo a decrease in the frequency of rain-on-snow (ROS) events; here the differing sensitivities were mostly explained by the current dominant phase of precipitation, the duration of snow cover and the average temperature. However, peak streamflows due to ROS

Table A1
Evaluation of CRHM model predictions of evapotranspiration, soil moisture, groundwater level, snow water equivalent, snow depth, snow covered area, snowcover duration, glacier mass balance, streamflow, water chemistry, and pond water level from publications using model runs and observations in Canada, China, Spain, Chile and Germany. Evaluation metrics include Nash–Sutcliffe efficiency (NSE), logarithmic NSE (logNSE), model bias (MB), root mean square difference (RMSD) or root mean square error (RMSE), normalised RMSD (NRMSD) or normalised RMSE (NRMSE), mean bias error (MBE), mean absolute error (MAE), Pearson product-moment correlation coefficient (r), coefficient of determination (r^2), Kling-Gupta efficiency (KGE), relative bias (Rbias), and Wang-Bovik Index (WBI).

Authors	Evaluation Variable	Evaluation Metrics											
		NSE	logNSE	MB	RMSD/ RMSE	NRMSD/ NRMSE	MBE	MAE	r	r^2	KGE	Rbias	WBI
	15-min evapotranspiration flux (mm 15 min^{-1})				0.014 to 0.019					0.61 to 0.78			
	Daily evapotranspiration flux (mm day^{-1})				0.54 to 0.91					0.22 to 0.66			
Armstrong et al. (2008)	Seasonal evaporation (mm)				2.31 to 5.07					0.9 to 0.98			
Armstrong et al. (2010)	Seasonal evapotranspiration (mm)			−0.17 to 0.07									
Aygün et al. (2020)	SWE (mm)	0.57		−0.1	28				0.84				
	Streamflow ($m^3 s^{-1}$)	0.51		0.024		0.7					0.71		
Cordeiro et al. (2017)	Streamflow ($m^3 s^{-1}$)	0.76		−0.31 to 0.5	0.51 to 2.31	0.89 to 1.34							
Costa et al. (2017)	SWE (mm)			−0.09 to 1.04									
	Streamflow (mm)			−0.28 to 0.45									
	NO_3 concentrations (mg l^{-1})	−7.03 to 0.97											
Costa et al. (2020)	Streamflow ($m^3 s^{-1}$)	−10.4 to 0.73		−0.76 to 1.73	0.03 to 0.25								
Costa et al. (2021)	Peak SWE (mm)	0.63 to 0.77		−0.03	3.55 to 4.93								
	Streamflow (l s^{-1})	−0.51 to 0.99		−0.62 to 1.19	0.01 to 4.52								
	NO_3 concentrations (mg l^{-1})	−2.42 to 0.16		−0.25 to 10.7	0.65 to 2.89								
	NH_4 concentrations (mg l^{-1})	−5.76 to 0.42		−0.38 to 0.08	0.76 to 2.02								
	SRP concentrations (mg l^{-1})	−35.45 to 0.94		−0.4 to 0.57	0.09 to 1.51								
	partP concentrations (mg l^{-1})	−0.23 to 0.43		0.16 to 25.91	0.16 to 2.78								
DeBeer and Pomeroy (2017)	Snow covered area (fraction)	0.9 to 0.94			0.09 to 0.12								
	Streamflow ($m^3 s^{-1}$)	0.46 to 0.58		−0.1 to −0.25	0.03 to 0.04								
Fang and Pomeroy (2007)	SWE (mm)	0.6 to 0.75		0.09 to 0.18									
	Streamflow ($m^3 s^{-1}$)	0.9		0.18									
Fang and Pomeroy (2008)	SWE (mm)			−0.28 to 0.18									
	Streamflow ($m^3 s^{-1}$)			−0.17 to 0.19									
Fang and Pomeroy (2009)	SWE (mm)	0.22 to 0.89		−0.37 to 0.23	2.06 to 30.61								
Fang et al. (2010)	SWE (mm)				1.7 to 25.2								
	Volumetric soil moisture (ratio)				0.009 to 0.011								
	Streamflow ($m^3 s^{-1}$)			−0.32 to −0.56	0.12 to 0.33								
Fang et al. (2013a,b)	SWE (mm)			−0.11 to 0.36	19.4 to 274.9	0.31 to 0.67							
	Volumetric soil moisture (ratio)			0.07 to 0.34	0.025 to 0.055	0.17 to 0.39							
	Groundwater level (m)								0.15 to 0.17				
	Streamflow ($m^3 s^{-1}$)	0.2 to 0.58		−0.29 to 0.01	0.036 to 0.147	0.6 to 0.76							

(continued on next page)

Table A1 (*continued*)

Authors	Evaluation Variable	Evaluation Metrics											
		NSE	logNSE	MB	RMSD/ RMSE	NRMSD/ NRMSE	MBE	MAE	r	r^2	KGE	Rbias	WBI
Fang and Pomeroy (2016)	Streamflow ($m^3 s^{-1}$)	0.71		−0.03	0.133	0.52							
He et al. (2021)	SWE (mm)			0.15 to 0.1		0.43 to 0.48							
	Evapotranspiration (mm)			0.03 to 0.11		0.61 to 0.74							
	Volumetric soil moisture (ratio)			−0.13 to 0.12		0.25 to 0.3							
	Streamflow ($m^3 s^{-1}$)	0.6 to 0.63	0.74 to 0.8	−0.12 to 0.04									
Krogh et al. (2015)	Streamflow ($m^3 s^{-1}$)	0.24 to 0.74		−0.3 to 1	60 to 101								
Krogh et al. (2017)	Streamflow ($m^3 s^{-1}$)	0.41		0.068 to 0.091									
	Soil active layer thickness (cm)			0.12				7.5					
López-Moreno et al. (2013)	Snow depth (cm)				36		−3.1						
	Snowpack duration (day)				15.1		7.8						
López-Moreno et al. (2014)	Snow depth (cm)						−0.39 to 0.14	0.21 to 0.41					
	Snowpack duration (day)						−12.6 to 12.5	11.4 to 16.8					
MacDonald et al. (2009)	SWE (mm)	0.04 to 0.98		−0.05 to 0.12	0.5 to 6.2								
MacDonald et al. (2010)	SWE (mm)	0.87 to 0.97		−0.01 to 0.13	5.1 to 13.2								
Mahmood et al. (2017)	Snow depth (cm)				7.2 to 10.01	0.42						−5% to −7%	
	Streamflow (mm day^{-1})	−0.1 to 0.48			0.74 to 1.44							−2% to 33 %	
Pomeroy et al. (2012a)	SWE (mm)					0.02 to 0.17							
	Streamflow ($m^3 s^{-1}$)	0.15											
Pomeroy et al. (2013)	Streamflow ($m^3 s^{-1}$)	0.41 to 0.87		−0.185 to 0.097									
Pomeroy et al. (2014)	SWE (mm)				8.1 to 49								
	Streamflow ($m^3 s^{-1}$)			−0.68 to 0.19	1.13 to 5.96								
Pomeroy et al. (2016)	SWE (mm)			0.17	93	0.43							
	Streamflow ($m^3 s^{-1}$)	0.54		−0.11	0.036	0.57							
Pradhananga and Pomeroy (2022)	Albedo (fraction)				0.117 to 0.17		−0.047 to 0.063						0.85 to 0.91
	Streamflow ($m^3 s^{-1}$)	0.56 to 0.77			1.09 to 1.87		−0.42 to 0.28						0.73 to 0.89
	Glacier mass balance (m)	0.424 to 0.998			0.27 to 0.8		−0.69 to 0.26						0.91 to 1
Rasouli et al. (2014)	SWE (mm)				29 to 35			23 to 28					
	Streamflow ($m^3 s^{-1}$)	0.15 to 0.49			0.72 to 0.88			0.44 to 0.49					
Rasouli et al. (2015)	SWE (mm)				50	0.046		26					
Rasouli et al. (2019)	SWE (mm)	0.18 to 0.93			19 to 131			14 to 97	0.73 to 0.98			−47 % to 5 %	
	Streamflow ($m^3 s^{-1}$)	0.4 to 0.71			0.008 to 0.75			0.003 to 0.37	0.7 to 0.87			−14 % to 28 %	
Sanmiguel-Vallelado et al. (2022)	SWE (mm)	0.85 to 0.96		−0.01 to 0.07	46 to 51								
	Peak SWE (mm)	0.8 to 0.94		−0.07 to −0.06	76 to 80								
	Snowpack duration (day)	0.67 to 0.9		−0.05 to 0.05	13 to 20								
Stone et al. (2019)	Snow depth (cm)	0.77 to 0.8		−0.318 to 0.203	10.1 to 11.7	0.452 to 0.479	−7.6 to 3.9						

(*continued on next page*)

Table A1 (*continued*)

Authors	Evaluation Variable	Evaluation Metrics NSE	logNSE	MB	RMSD/ RMSE	NRMSD/ NRMSE	MBE	MAE	r	r^2	KGE	Rbias	WBI
										0.86 to 0.91			
	SWE (mm)			0.017 to 0.235	18.2 to 37.1	0.404 to 1.549	2 to 30.8			0.65 to 0.78			
	Evapotranspiration flux (mm hour^{-1})			0.101 to 0.479	0.058 to 0.089	0.737 to 0.892	0.012 to 0.067			0.53 to 0.75			
	Pond water level (mm)			0.714	50.2	0.754	21.3						
Van Hoy et al. (2020)	SWE (mm)	0.7										4.3 %	
	Streamflow (m^3 s^{-1})	0.5										3.6 %	
Weber et al. (2016)	Snow depth (cm)	0.53			77								
Zhou et al. (2014)	SWE (mm)				12.4		0.3			0.78			
	Streamflow (m^3 s^{-1})	0.76 to 0.79								0.83 to 0.87			

are projected to be more intense as a consequence of higher energy inputs, and more common isothermal snowpack energy state. This type of virtual basin analysis proved to be a good complement to studies performed in mountain research basins with in-situ measured meteorological forcing, as the virtual basin approach facilitated isolating the effects of differing climatic conditions on the response of snow and hydrology to climate warming.

6. Conclusions

The Cold Regions Hydrological Modelling platform (CRHM) was devised as a tool to better understand the significance of process hydrology investigations in research basins for generation of snowpacks, glaciers, soil moisture, evapotranspiration, wetlands and streamflow, and has also shown capabilities to assess the impacts of climate and land use change on hydrology. The CRHM platform allows for multiple representations of forcing data interpolation and extrapolation, hydrological model spatial and physical process structure and parameter values with reproducible workflows for each unique model creation. It is well suited for model falsification, algorithm benchmarking, model mimicry and intercomparison, and has been deployed for basin hydrology diagnosis, prediction, land use change analysis, water quality, climate impact analysis and flood forecasting. The development of additional hydrological processes in CRHM has been through the incorporation and inclusion of process modules developed by scientists after intensive study of cold regions and other hydrological processes in research basins. CRHM's capabilities permit the development of hydrological insights through model diagnosis of the role of hydrological processes in controlling snowpack, glacier, soil moisture, evapotranspiration, soil thaw, groundwater, runoff, water quality and streamflow regimes. Examples presented here demonstrate how the regional hydrological diagnosis approaches can be applied for hydrological science investigations and to compare environments over global extents to diagnose cryospheric and hydrological dynamics and their response to disturbance such as climate change and land cover change. Modelling experiments in CRHM to examine hydrological processes, model structure and parameterisation have helped to better understand why temperate zone hydrological models have often failed to represent cold regions basin hydrology adequately and the importance of snow, glacier and frozen ground processes for representation of the hydrology of cold regions and seasons. The model has recently been re-engineered to permit platform independence and accelerated calculation, and will soon have the ability to use model agnostic automated basin delineation and parameter identification and further development of capabilities for northern peatland evaporation, beaver pond water storage, sediment erosion and dissolved organic carbon export, infiltration to frozen soils on slopes and rock glacier hydrology. It is hoped that CRHM's story can inspire developments in other hydrological modelling programmes to include structural flexibility, snow and ice processes, process realism, multiphysics approaches, uncalibrated parameterisation and strong interactions with field hydrology studies as these have proven scientifically and practically beneficial in the development and application of CRHM to the science of hydrology.

CRediT authorship contribution statement

J.W. Pomeroy: Conceptualization, Formal analysis, Funding acquisition, Investigation, Methodology, Supervision, Writing – original draft, Writing – review & editing. **T. Brown:** Data curation, Investigation, Formal analysis, Software, Validation. **X. Fang:** Data curation, Formal analysis, Investigation, Methodology, Software, Visualisation, Writing – original draft, Writing – review & editing. **K.R. Shook:** Conceptualization, Data curation, Formal analysis, Investigation, Methodology, Software,Writing – original draft, Writing – review & editing. **D. Pradhananga:** Investigation, Methodology, Writing – original draft. **R. Armstrong:** Investigation, Methodology, Writing – original draft. **P. Harder:** Investigation, Formal analysis, Writing – original draft. **C. Marsh:** Data curation, Software, Writing – original draft. **D. Costa:** Formal analysis, Investigation, Software, Writing – original draft. **S.A. Krogh:** Formal analysis, Writing – original draft. **C. Aubry-Wake:** Formal analysis, Investigation, Writing – original draft. **H. Annand:** Methodology, Writing – review & editing. **P. Lawford:** Software, Data curation, Writing – review & editing. **Z. He:** Formal analysis, Investigation, Writing – original draft. **M. Kompanizare:** Formal analysis, Investigation, Software, Validation, Writing – original draft. **I. Lopez Moreno:** Investigation, Visualization, Writing – original draft.

Declaration of Competing Interest

The authors declare that they have no known competing financial interests or personal relationships that could have appeared to influence the work reported in this paper.

Data availability

The authors are unable or have chosen not to specify which data has been used.

Acknowledgements

The authors wish to acknowledge the cold regions science developments in many institutions, including the Division of Hydrology, University of Saskatchewan under the direction of the late Professor Donald M. Gray, that have been incorporated into CRHM. We also note the 50-year hydrological modelling career of Mr. Tom Brown of the Division of Hydrology and later Centre for Hydrology that led to the development and growth of this model. This is notwithstanding the contributions of dozens of students and colleagues from Canada, UK, Spain, USA, China, Chile, Germany, Austria, Russia, Nepal and elsewhere to the model development. Funding for the model has come from many sources, principally the Natural Sciences and Engineering Research Council of Canada, Environment Canada, Indian and Northern Affairs Canada, Yukon Environment, the Forest Resource Improvement Association of Alberta, Alberta Agriculture and Forestry, Alberta Environment, Ducks Unlimited Canada, Water Security Agency of Saskatchewan, Natural Environment Research Council (UK), IPE-CSIC (Spain), Canada Research Chair and Canada Excellence Research Chairs programmes, and the Canada First Research Excellence Fund's Global Water Futures programme. This manuscript was completed whilst on sabbatical as a guest of CSIC-IPE in the Pyrenees, where many innovative applications of the model have been made.

Code and Utility Availability

The model, manual, and related publications can be found here https://research-groups.usask.ca/hydrology/modelling/crhm.php, and source code, example models and some utilities for importing data into CRHM can be found here https://github.com/CentreForHydrology/crhm.

Appendix

References

Anderson, D.L.L., Benson, C.S.S., 1963. The densification and diagenesis of snow. Ice and Snow: Properties, Processes and Applications Properties, Processes and Applications. MIT Press, Cambridge, MA, 391–411.

Annandale, J.G., Jovanovic, N.Z., Benadé, N., Allen, R.G., 2001. Software for missing data analysis of Penman-Monteith reference evapotranspiration. Irrigation Sci. 21, 57–67.

Armstrong, R.N., Pomeroy, J.W., Martz, L.W., 2008. Evaluation of three evaporation estimation methods in a Canadian prairie landscape. Hydrol. Process. 22, 2801–2815.

Armstrong, R.N., Pomeroy, J.W., Martz, L.W., 2010. Estimating evaporation in a Prairie landscape under drought conditions. Can. Water Resour. J. 35 (2), 173–186. https://doi.org/10.4296/cwrj3502173.

Aygün, O., Kinnard, C., Campeau, S., Krogh, S.A., 2020. Shifting hydrological processes in a Canadian agroforested catchment due to a warmer and wetter climate. Water 12, 739. https://doi.org/10.3390/w12030739.

Bash, E.A., Marshall, S.J., 2014. Estimation of glacial melt contributions to the Bow River, Alberta, Canada, using a radiation-temperature melt model. Ann. Glaciol. 55 (66), 138–152. https://doi.org/10.3189/2014AoG66A226.

Baulch, H.M., Elliott, J.A., Cordeiro, M.R.C., Flaten, D.N., Lobb, D.A., Wilson, H.F., 2019. Soil and water management: opportunities to mitigate nutrient losses to surface waters in the Northern Great Plains. Environ. Rev. 27 (4), 447–477. https://doi.org/10.1139/er-2018-0101.

Bernhardt, M., Schulz, K., 2010. SnowSlide: A simple routine for calculating gravitational snow transport. Geophys. Res. Lett. 37, L11502. https://doi.org/10.1029/2010GL043086.

Beven, K., 1993. Prophecy, reality and uncertainty in distributed hydrological modelling. Adv. Water Resour. 16, 41–51. https://doi.org/10.1016/0309-1708(93)90028-E.

Bolch, T., Menounos, B., Wheate, R., 2010. Landsat-based inventory of glaciers in western Canada, 1985–2005. Remote Sens. Environ. 114 (1), 127–137.

Bring, A., Fedorova, I., Dibike, Y., Hinzman, L., Mård, J., Mernild, S.H., Woo, M.-K., 2016. Arctic terrestrial hydrology: A synthesis of processes, regional effects, and research challenges. J. Geophys. Res.-Biogeo. 121, 621–649. https://doi.org/10.1002/2015JG003131.

Brooks, R.H., Corey, A.T., 1964. Hydraulic Properties of Porous Media. Hydrology Papers 3. Colorado State University, Fort Collins, Colorado, 27.

Brooks, P.D., Williams, M.W., Schmidt, S.K., 1996. Microbial activity under alpine snowpacks, Niwot Ridge, Colorado. Biogeochemistry 32 (2), 93–113.

Broughton, R., Jutras, P., 2013. Farm Drainage. In The Canadian Encyclopedia. Retrieved from https://www.thecanadianencyclopedia.ca/en/article/farm-drainage.

Brutsaert, W., 1982. Evaporation into the Atmosphere: Theory, History, and Applications. D. Reidel Publishing Company, Dordrecht.

Cade-Menun, B.J., Bell, G., Baker-Ismail, S., Fouli, Y., Hodder, K., McMartin, D.W., Wu, K., 2013. Nutrient loss from Saskatchewan cropland and pasture in spring snowmelt runoff. Can. J. Soil Sci. 93 (4), 445–458.

Carenzo, M., Pellicciotti, F., Mabillard, J., Reid, T., Brock, B.W., 2016. An enhanced temperature index model for debris-covered glaciers accounting for thickness effect. Adv. Water Resour. 94, 457–469.

Carey, S.K., Woo, M., 2005. Freezing of subarctic hillslopes, Wolf Creek Basin, Yukon, Canada. Arct. Antarct. Alp. Res. 37 (1), 1–10.

Chow, V.T., 1964. Handbook of Applied Hydrology. McGraw-Hill Inc, New York.

Clark, C.O., 1945. Storage and the unit hydrograph. Proc. Am. Soc. Civil Eng. 69, 1419–1447.

Clark, K., Chantigny, M.H., Angers, D.A., Rochette, P., Parent, L.É., 2009. Nitrogen transformations in cold and frozen agricultural soils following organic amendments. Soil Biol. Biochem. 41 (2), 348–356.

Clarke, G.K.C., Jarosch, A.H., Anslow, F.S., Radić, V., Menounos, B., 2015. Projected deglaciation of western Canada in the twenty-first century. Nat. Geosci. 8, 372–377. https://doi.org/10.1038/ngeo2407.

Cober, J.R., Macrae, M.L., Van Eerd, L.L., 2018. Nutrient release from living and terminated cover crops under variable freeze–thaw cycles. Agron. J. 110, 1036–1045. https://doi.org/10.2134/agronj2017.08.0449.

Comeau, L.E.L., Pietroniro, A., Demuth, M.N., 2009. Glacier contribution to the North and South Saskatchewan Rivers. Hydrol. Process. 23 (18), 2640-2653. doi:10.1002/hyp.7409.

Connon, R.F., Quinton, W.L., Craig, J.R., Hayashi, M., 2014. Changing hydrologic connectivity due to permafrost thaw in the lower Liard River valley, NWT, Canada. Hydrol. Process. 28 (14), 4163–4178. https://doi.org/10.1002/hyp.10206.

Cordeiro, M.R.C., Wilson, H.F., Vanrobaeys, J., Pomeroy, J.W., Fang, X., The Red-Assiniboine Project Biophysical Modelling Team, 2017. Simulating cold-region hydrology in an intensively drained agricultural watershed in Manitoba, Canada, using the Cold Regions Hydrological Model. Hydrol. Earth Syst. Sc. 21, 3483–3506. https://doi.org/10.5194/hess-21-3483-2017.

Costa, D., Shook, K., Spence, C., Elliott, J., Baulch, H., Wilson, H., Pomeroy, J., 2020. Predicting variable contributing areas, hydrological connectivity, and solute transport pathways for a Canadian Prairie basin. Water Resour. Res. 56, e2020WR027984. doi:10.1029/2020WR027984.

Costa, D., Roste, J., Pomeroy, J., Baulch, H., Elliot, J., Wheater, H., Westbrook, C., 2017. A modelling framework to simulate field-scale nitrate response and transport during snowmelt: The WINTRA model. Hydrol. Process. 31, 4250–4268. https://doi.org/10.1002/hyp.11346.

Costa, D., Pomeroy, J., Baulch, H., Elliot, J., Wheater, H., 2019. Using an inverse modelling approach with equifinality control to investigate the dominant controls on snowmelt nutrient export. Hydrol. Process. 33, 2958–2977. https://doi.org/10.1002/hyp.13463.

Costa, D., Pomeroy, J.W., Brown, T., Baulch, H., Elliott, J., Macrae, M., 2021. Advances in the simulation of nutrient dynamics in cold climate agricultural basins: Developing new nitrogen and phosphorus modules for the Cold Regions Hydrological Modelling Platform. J. Hydrol. 603, 126901 https://doi.org/10.1016/j.jhydrol.2021.126901.

DeBeer, C.M., Pomeroy, J.W., 2017. Influence of snowpack and melt energy heterogeneity on snow cover depletion and snowmelt runoff simulation in a cold mountain environment. J. Hydrol. 553, 199–213. https://doi.org/10.1016/j.jhydrol.2017.07.051.

Demuth, M., Pinard, V., Pietroniro, A., Luckman, B., Hopkinson, C., Dornes, P., Comeau, L., 2008. Recent and past-century variations in the glacier resources of the Canadian Rocky Mountains: Nelson River system. Terra Glacialis Special Issue – Mountain Glaciers and Climate Changes of the Last Century, 27-52.

Dornes, P.F., Pomeroy, J.W., Pietroniro, A., Carey, S.K., Quinton, W.L., 2008. Influence of landscape aggregation in modelling snow-cover ablation and snowmelt runoff in a sub-arctic mountainous environment. Hydrolog. Sci. J. 53 (4), 725–740.

Dumanski, S., Pomeroy, J.W., Westbrook, C.J., 2015. Hydrological regime changes in a Canadian Prairie basin. Hydrol. Process. 29, 3893–3904. https://doi.org/10.1002/hyp.10567.

Duncan, E.W., King, K.W., Williams, M.R., LaBarge, G., Pease, L.A., Smith, D.R., Fausey, N.R., 2017. Linking soil phosphorus to dissolved phosphorus losses in the Midwest. Agric. Environ. Lett. 2 (1), 170004 https://doi.org/10.2134/ael2017.02.0004.

Dyck, G.E., Gray, D.M., Brown, T., 1974. Areal Variability of Precipitation in the Bad Lake Watershed, Saskatchewan, Division of Hydrology Report, Progress Report 1973/74. Division of Hydrology, University of Saskatchewan, Saskatoon, Canada.

Elliott, J., 2013. Evaluating the potential contribution of vegetation as a nutrient source in snowmelt runoff. Can. J. Soil Sci. 93 (4), 435–443.

Ellis, C.R., Pomeroy, J.W., Brown, T., MacDonald, J., 2010. Simulation of snow accumulation and melt in needleleaf forest environments. Hydrol. Earth Syst. Sc. 14, 925–940.

Essery, R., Etchevers, P., 2004. Parameter sensitivity in simulations of snowmelt. J. Geophys. Res. 109, D20111. https://doi.org/10.1029/2004JD005036.

Fang, X., Pomeroy, J.W., (n.d.). Simulation of future changes in climate and glacier cover on the hydrology of Bow River headwater basins in the Canadian Rockies. In preparation.

Fang, X., Pomeroy, J.W., 2007. Snowmelt runoff sensitivity analysis to drought on the Canadian prairies. Hydrol. Process. 21 (19), 2594–2609. https://doi.org/10.1002/hyp.6796.

Fang, X., Pomeroy, J.W., 2008. Drought impacts on Canadian prairie wetland snow hydrology. Hydrol. Process. 22, 2858–2873. https://doi.org/10.1002/hyp.7074.

Fang, X., Pomeroy, J.W., 2009. Modelling blowing snow redistribution to prairie wetlands. Hydrol. Process. 23 (18), 2557–2569. https://doi.org/10.1002/hyp.7348.

Fang, X., Pomeroy, J.W., Westbrook, C.J., Guo, X., Minke, A.G., Brown, T., 2010. Prediction of snowmelt derived streamflow in a wetland dominated prairie basin. Hydrol. Earth Syst. Sc. 14 (6), 991–1006. https://doi.org/10.5194/hess-14-991-2010.

Fang, X., Pomeroy, J.W., 2020. Diagnosis of future changes in hydrology for a Canadian Rockies headwater basin. Hydrol. Earth Syst. Sc. 24 (5), 2731–2754. https://doi.org/10.5194/hess-24-2731-2020.

Fang, X., Pomeroy, J.W., Ellis, C.R., MacDonald, M.K., DeBeer, C.M., Brown, T., 2013a. Multi-variable evaluation of hydrological model predictions for a headwater basin in the Canadian Rocky Mountains. Hydrol. Earth Syst. Sc. 17, 1635–1659. https://doi.org/10.5194/hess-17-1635-2013.

Fang, X., Pomeroy, J.W., Ellis, C.R., MacDonald, M.K., DeBeer, C.M., Brown, T., 2013b. Multi-variable evaluation of hydrological model predictions for a headwater basin in the Canadian Rocky Mountains. Hydrol. Earth Syst. Sc. 17 (4), 1635–1659. https://doi.org/10.5194/hess-17-1635-2013.

Fox, J.D., 1992. Incorporating freeze-thaw calculations into a water balance model. Water Resour. Res. 28 (9), 2229–2244. https://doi.org/10.1029/92WR00983.

Freeze, R.A., Cherry, J.A., 1979. Groundwater. Prentice Hall Inc, New Jersey.

Garnier, B.J., Ohmura, A., 1970. The evaluation of surface variations in solar radiation income. Sol. Energy 13 (1), 21–34.

Gleick, P.H., 1986. Methods for evaluating the regional hydrologic impacts of global climatic changes. J. Hydrol. 88, 97–116. https://doi.org/10.1016/0022-1694(86)90199-X.

Goodison, B.E., Louie, P.Y.T., Yang, D., 1998. WMO Solid Precipitation Measurement Intercomparison Final Report (WMO Instruments and Observing Methods Report No. 67). Retrieved from https://www.wmo.int/pages/prog/www/reports/WMOtd872.pdf.

Graham, C.B., Woods, R.A., McDonnell, J.J., 2010. Hillslope threshold response to rainfall: (1) A field based forensic approach. J. Hydrol. 393 (1–2), 65–76. https://doi.org/10.1016/j.jhydrol.2009.12.015.

Granger, R.J., Gray, D.M., 1989. Evaporation from natural nonsaturated surfaces. J. Hydrol. 111, 21–29.

Grant, K.N., Macrae, M.L., Ali, G.A., 2019. Differences in preferential flow with antecedent moisture conditions and soil texture: Implications for subsurface P transport. Hydrol. Process. 33 (15), 2068–2079. https://doi.org/10.1002/hyp.13454.

Gray, D.M., Granger, R.J., 1988. Bad Lake Watershed: 1967 – 1986. In: Canadian Hydrology Symposium, Associate Committee on Hydrology, National Research Council of Canada, Banff, Alberta, 9-11 May 1988, pp. 143-153.

Gray, D.M., Pomeroy, J.W., Granger, R.J., 1986. Prairie Snowmelt Runoff. In: Proceedings of Water Research Themes, Conference Commemorating the Official Opening of the National Hydrology Research Centre, Saskatoon, Saskatchewan, pp. 49-68.

Gray, D.M., Landine, P.G., 1987. Albedo model for shallow prairie snow covers. Can. J. Earth Sci. 24, 1760–1768.

Gray, D.M., Landine, P.G., 1988. An energy-budget snowmelt model for the Canadian Prairies. Can. J. Earth Sci. 25, 1292–1303.

Gray, D.M., Toth, B., Zhao, L., Pomeroy, J.W., Granger, R.J., 2001. Estimating areal snowmelt infiltration into frozen soils. Hydrol. Process. 15, 3095–3111.

Haghnazari, F., Karandish, F., Darzi-Naftchali, A., Šimůnek, J., 2020. Dynamic assessment of the impacts of global warming on nitrate losses from a subsurface-drained rainfed-canola field. Agr. Water Manage. 242, 106420 https://doi.org/10.1016/j.agwat.2020.106420.

Hannah, D.M., Gurnell, A.M., 2001. A conceptual, linear reservoir runoff model to investigate melt season changes in cirque glacier hydrology. J. Hydrol. 246, 123–141. https://doi.org/10.1016/S0022-1694(01)00364-X.

Harder, P., Pomeroy, J.W., 2013. Estimating precipitation phase using a psychrometric energy balance method. Hydrol. Process. 27, 1901–1914. https://doi.org/10.1002/hyp.9799.

Harder, P., Pomeroy, J.W., 2014. Hydrological model uncertainty due to precipitation phase partitioning methods. Hydrol. Process. 28, 4311–4327. https://doi.org/10.1002/hyp.10214.

Harder, P., Pomeroy, J.W., Westbrook, C.J., 2015. Hydrological resilience of a Canadian Rockies headwaters basin subject to changing climate, extreme weather, and forest management. Hydrol. Process. 29, 3905–3924. https://doi.org/10.1002/hyp.10596.

Harpold, A.A., Kaplan, M.L., Klos, P.Z., Link, T.E., Mcnamara, J.P., Rajagopal, S., Schumer, R., Steele, C.M., 2017. Rain or snow : hydrologic processes, observations, prediction, and research needs. Hydrol. Earth Syst. Sc. 21 (1), 1–22. https://doi.org/10.5194/hess-21-1-2017.

Hay, L.E., Wilby, R.L., Leavesley, G.H., 2000. A Comparison of Delta Change and Downscaled GCM Scenarios for three Mountainous Basins in the United States. J. Am. Water Resour. As. 36, 387–397.

Hayashi, M., 2020. Alpine hydrogeology: The critical role of groundwater in sourcing the headwaters of the world. Groundwater 58 (4), 498–510. https://doi.org/10.1111/gwat.12965.

Hayashi, M., Goeller, N., Quinton, W.L., Wright, N., 2007. A simple heat-conduction method for simulating the frost-table depth in hydrological models. Hydrol. Process. 21 (19), 2610–2622. doi:10.1002/(ISSN)1099-108510.1002/hyp.v21: 1910.1002/hyp.6792.

He, Z., Pomeroy, J.W., Fang, X., Peterson, A., 2021. Sensitivity analysis of hydrological processes to perturbed climate in a southern boreal forest basin. J. Hydrol. 601, 126706 https://doi.org/10.1016/j.jhydrol.2021.126706.

Hedstrom, N.R., Pomeroy, J.W., 1998. Measurements and modelling of snow interception in the boreal forest. Hydrol. Process. 12, 1611–1625.

Hjort, J., Karjalainen, O., Aalto, J., Westermann, S., Romanovsky, V.E., Nelson, F.E., Etzelmuller, B., Luoto, M., 2018. Degrading permafrost puts Arctic infrastructure at risk by mid-century. Nat. Commun. 9, 5147. https://doi.org/10.1038/s41467-018-07557-4.

Hooghoudt, S.B., 1940. Bijdrage tot de kennis van enige Natuurkundige Grootheden van de Grand. Verslagen van Landbouwkundige Onderzoekingen 46 (7), 515-707. The Hague, The Netherlands (in Dutch).

Hopkinson, C., Young, G.J., 1998. The effect of glacier wastage on the flow of the Bow River at Banff, Alberta, 1951–1993. Hydrol. Process. 12 (10–11), 1745–1762.

Hrachowitz, M., Clark, M.P., 2017. HESS Opinions: The complementary merits of competing modelling philosophies in hydrology. Hydrol. Earth Syst. Sc. 21, 3953–3973. https://doi.org/10.5194/hess-21-3953-2017.

ICID, 2018. World Drained Area – 2018. International Commission on Irrigation and Drainage. Retrieved from http://www.icid.org/world-drained-area.pdf.

Irvine, C., Macrae, M., Morison, M., Petrone, R., 2019. Seasonal nutrient export dynamics in a mixed land use subwatershed of the Grand River, Ontario, Canada. J. Great Lakes Res. 45 (6), 1171–1181. https://doi.org/10.1016/j.jglr.2019.10.005.

Jennings, K.S., Winchell, T.S., Livneh, B., Molotch, N.P., 2018. Spatial variation of the rain-snow temperature threshold across the Northern Hemisphere. Nat. Commun. 9, 1148. https://doi.org/10.1038/s41467-018-03629-7.

Jones, H.G., 1999. The ecology of snow-covered systems: A brief overview of nutrient cycling and life in the cold. Hydrol. Process. 13 (14–15), 2135–2147.

Jones, H.G., 1987. Chemical dynamics of snow cover and snowmelt in a boreal forest, in: Jones, H.G., Orville-Thomas, W.J. (Eds.), Seasonal Snow Covers: Physics, Chemistry, Hydrology. NATO-ASI series C: Mathematical and physical sciences, vol 211, pp. 531-574. Springer, Dordrecht. doi:10.1007/978-94-009-3947-9_24.

Kane, D.L., Stein, J., 1983. Water movement into seasonally frozen soils. Water Resour. Res. 19 (6), 1547–1557.

Keith, D.M., Johnson, E.A., Valeo, C., 2010. A hillslope forest floor (duff) water budget and the transition to local control. Hydrol. Process. 24 (19), 2738–2751. https://doi.org/10.1002/hyp.7697.

Kirkby, M., 1988. Hillslope runoff processes and models. J. Hydrol. 100 (1–3), 315–339.

Knoben, W.J.M., Clark, M.P., Bales, J., Bennett, A., Gharari, S., Marsh, C.B., Nijssen, B., et al. 2021. Community Workflows to Advance Reproducibility in Hydrologic Modeling: Separating Model-Agnostic and Model-Specific Configuration Steps in Applications of Large-Domain Hydrologic Models. Submitted to Wat. Res. Res., Earth and Space Science Open Archive. doi:10.1002/essoar.10509195.1.

Kokulan, V., Macrae, M.L., Lobb, D.A., Ali, G.A., 2019. Contribution of Overland and Tile Flow to Runoff and Nutrient Losses from Vertisols in Manitoba, Canada. J. Environ. Qual. 48, 959–965. https://doi.org/10.2134/jeq2019.03.0103.

Kompanizare, M., Costa, D., Macrae, M., Pomeroy, J.W., Petrone, R., in eview. Developing a tile drainage module for Cold Region Hydrological Model: Lessons from a farm in Southern Ontario, Canada. J. Hydrol. HYDROL44875.

Krinner, G., Derksen, C., Essery, R., Flanner, M., Hagemann, S., Clark, M., Zhu, D., 2018. ESM-Snow MIP: assessing snow models and quantifying snow-related climate feedbacks. Geosci. Model Dev. 11, 5027–5049. https://doi.org/10.5194/gmd-11-5027-2018.

Krogh, S., Pomeroy, J., Mcphee, J., 2015. Physically Based Mountain Hydrological Modeling Using Reanalysis Data in Patagonia. J. Hydrometeorol. 16, 172–193. https://doi.org/10.1175/JHM-D-13-0178.1.

Krogh, S.A., Pomeroy, J.W., 2018. Recent changes to the hydrological cycle of an Arctic basin at the tundra–taiga transition. Hydrol. Earth Syst. Sc. 22 (7), 3993–4014. https://doi.org/10.5194/hess-22-3993-2018.

Krogh, S.A., Pomeroy, J.W., 2021. Simulating site-scale permafrost hydrology: Sensitivity to modelling decisions and air temperature. J. Hydrol. 602, 126771 https://doi.org/10.1016/j.jhydrol.2021.126771.

Krogh, S.A., Pomeroy, J.W., Marsh, P., 2017. Diagnosis of the hydrology of a small Arctic basin at the tundra-taiga transition using a physically based hydrological model. J. Hydrol. 550, 685–703. https://doi.org/10.1016/j.jhydrol.2017.05.042.

Kurylyk, B.L., McKenzie, J.M., MacQuarrie, K.T.B., Voss, C.I., 2014. Analytical solutions for benchmarking cold regions subsurface water flow and energy transport models: One-dimensional soil thaw with conduction and advection. Adv. Water Resour. 70, 172–184. https://doi.org/10.1016/j.advwatres.2014.05.005.

Lam, W.V., Macrae, M.L., English, M.C., O'Halloran, I.P., Wang, Y.T., 2016. Effects of tillage practices on phosphorus transport in tile drain effluent under sandy loam agricultural soils in Ontario, Canada. J. Great Lakes Res. 42 (6), 1260–1270.

Laudon, H., Spence, C., Buttle, J., Carey, S.K., McDonnell, J.J., McNamara, J.P., Soulsby, C., Tetzlaff, D., 2017. Save northern high-latitude catchments. Nat. Geosci. 10 (5), 324–325. https://doi.org/10.1038/ngeo2947.

Leavesley, G.H., Lichty, R.W., Troutman, B.M., Saindon, L.G., 1983. Precipitation-runoff modelling system: User's manual. Report 83–4238. US Geological Survey Water Resources Investigations, Washington DC, US.

Li, H., Beldring, S., Xu, C.-Y., Huss, M., Melvold, K., Jain, S.K., 2015. Integrating a glacier retreat model into a hydrological model – Case studies of three glacierised catchments in Norway and Himalayan region. J. Hydrol. 527, 656–667. https://doi.org/10.1016/j.jhydrol.2015.05.017.

Li, Y., Li, Z., Zhang, Z., Chen, L., Kurkute, S., Scaff, L., Pan, X., 2019. High-resolution regional climate modeling and projection over Western Canada using a Weather Research Forecasting model with a pseudo-global warming approach. Hydrol. Earth Syst. Sc. 23 (11), 4635–4659. https://doi.org/10.5194/hess-23-4635-2019.

Li, L., Pomeroy, J.W., 1997. Probability of occurrence of blowing snow. J. Geophys. Res. 102, 21955–21964.

Lindström, G., Pers, C., Rosberg, J., Strömqvist, J., Arheimer, B., 2010. Development and testing of the HYPE (Hydrological Predictions for the Environment) water quality model for different spatial scales. Hydrol. Res. 41 (3–4), 295–319. https://doi.org/10.2166/nh.2010.007.

Ling, F., Zhang, T., 2004. A numerical model for surface energy balance and thermal regime of the active layer and permafrost containing unfrozen water. Cold Reg. Sci. Technol. 38 (1), 1–15.

Lique, C., Holland, M.M., Dibike, Y.B., Lawrence, D.M., Screen, J.A., 2016. Modeling the Arctic freshwater system and its integration in the global system: lessons learned and future challenges. J. Geophys. Res.-Biogeo. 121 (3), 540–566. https://doi.org/10.1002/2015JG003120.

Liu, K., Elliott, J.A., Lobb, D.A., Flaten, D.N., Yarotski, J., 2013. Critical factors affecting field-scale losses of nitrogen and phosphorus in spring snowmelt runoff in the Canadian Prairies. J. Environ. Qual. 42 (2), 484–496.

Liu, K., Elliott, J.A., Lobb, D.A., Flaten, D.N., Yarotski, J., 2014. Nutrient and sediment losses in snowmelt runoff from perennial forage and annual cropland in the Canadian Prairies. J. Environ. Qual. 43 (5), 1644–1655.

Liu, J., Macrae, M.L., Elliott, J.A., Baulch, H.M., Wilson, H.F., Kleinman, P.J., 2019. Impacts of Cover Crops and Crop Residues on Phosphorus Losses in Cold Climates: A Review. J. Environ. Qual. 48, 850–868. https://doi.org/10.2134/jeq2019.03.0119.

López-Moreno, J.I., Pomeroy, J.W., Revuelto, J., Vicente-Serrano, S.M., 2013. Response of snow processes to climate change: Spatial variability in a small basin in the Spanish Pyrenees. Hydrol. Process. 27 (18), 2637–2650. https://doi.org/10.1002/hyp.9408.

López-Moreno, J.I., Revuelto, J., Gilaberte, M., Morán-Tejeda, E., Pons, M., Jover, E., Esteban, P., Garcia, C., Pomeroy, J., 2014. The effect of aspect on the response of snowpack to climate warming in the Pyrenees. Theor. Appl. Climatol. 117, 207–219. https://doi.org/10.1007/s00704-013-0991-0.

López-Moreno, J.I., Boike, J., Sanchez-Lorenzo, A., Pomeroy, J.W., 2016. Impact of climate warming on snow processes in Ny-Ålesund, a polar maritime site at Svalbard. Global Planet. Change 146, 10–21. https://doi.org/10.1016/j.gloplacha.2016.09.006.

López-Moreno, J.I., Gascoin, S., Herrero, J., Sproles, E.A., Pons, M., Alonso-González, E., Pomeroy, J., 2017. Different sensitivities of snowpacks to warming in Mediterranean climate mountain areas. Environ. Res. Lett. 12 (7), 074006 https://doi.org/10.1088/1748-9326/aa70cb.

López-Moreno, J.I., Pomeroy, J.W., Alonso-González, E., Morán-Tejeda, E., Revuelto, J., 2020. Decoupling of warming mountain snowpacks from hydrological regimes. Environ. Res. Lett. 15 (11), 114006 https://doi.org/10.1088/1748-9326/abb55f.

López-Moreno, J.I., Pomeroy, J.W., Morán-Tejeda, E., Revuelto, J., Navarro-Serrano, F. M., Vidaller, I., Alonso-González, E., 2021. Changes in the frequency of global high mountain rain-on-snow events due to climate warming. Environ. Res. Lett. 16 (9), 94021. https://doi.org/10.1088/1748-9326/ac0dde.

Luce, C.H., Tarboton, D.G., 2010. Evaluation of alternative formulae for calculation of surface temperature in snowmelt models using frequency analysis of temperature observations. Hydrol. Earth Syst. Sc. 14 (3), 535–543. https://doi.org/10.5194/hess-14-535-2010.

Lunardini, V.J., 1998. Effect of convective heat transfer on thawing of frozen soil. In: Lewkowicz AG, Allard M, editors. Proceedings of the Seventh International Conference on Permafrost. Canada: Yellowknife. p. 689–95.

Lv, Z., Pomeroy, J.W., Fang, X., 2019. Evaluation of SNODAS snow water equivalent in Western Canada and assimilation into a cold region hydrological model. Water Resourc. Res. 55, 11166–11187. https://doi.org/10.1029/2019WR02533.

MacDonald, M.K., Pomeroy, J.W., Pietroniro, A., 2009. Parameterizing redistribution and sublimation of blowing snow for hydrological models: tests in a mountainous subarctic catchment. Hydrol. Process. 23, 2570–2583. https://doi.org/10.1002/hyp.7356.

MacDonald, M.K., Pomeroy, J.W., Pietroniro, A., 2010. On the importance of sublimation to an alpine snow mass balance in the Canadian Rocky Mountains. Hydrol. Earth Syst. Sc. 14, 1401–1415. https://doi.org/10.5194/hess-14-1401-2010.

Macrae, M.L., English, M.C., Schiff, S.L., Stone, M., 2007. Intra-annual variability in the contribution of tile drains to basin discharge and phosphorus export in a first-order agricultural catchment. Agr. Water Manage. 92 (3), 171–182.

Macrae, M.L., Ali, G.A., King, K.W., Plach, J.M., Pluer, W.T., Williams, M., Morison, M. Q., Tang, W., 2019. Evaluating Hydrologic Response in Tile-Drained Landscapes: Implications for Phosphorus Transport. J. Environ. Qual. 48, 1347–1355. https://doi.org/10.2134/jeq2019.02.0060.

Mahmood, T.H., Pomeroy, J.W., Wheater, H.S., Baulch, H.M., 2017. Hydrological responses to climatic variability in a cold agricultural region. Hydrol. Process. 31, 854–870. https://doi.org/10.1002/hyp.11064.

Male, D.H., Gray, D.M., 1981. Snowcover ablation and runoff. In: Gray, D.M., Male, D.H. (Eds.), Handbook of Snow. Pergamon Press, Toronto, pp. 360–436.

Marks, D., Dozier, J., 1992. Climate and energy exchange at the snow surface in the alpine region of the Sierra Nevada: 2. Snow cover energy balance. Water Resour. Res. 28, 3043–3054.

Marks, D., Kimball, J., Tingey, D., Link, T., 1998. The sensitivity of snowmelt processes to climate conditions and forest cover during rain-on-snow: a case study of the 1996 Pacific Northwest flood. Hydrol. Process. 12, 1569–1587.

Marks, D., Winstral, A., Reba, M., Pomeroy, J.W., Kumar, M., 2013. An evaluation of methods for determining during-storm precipitation phase and the rain/snow transition elevation at the surface in a mountain basin. Adv. Water Resour. 55, 98–110. https://doi.org/10.1016/j.advwatres.2012.11.012.

Marsh, C.B., Pomeroy, J.W., Wheater, H.S., 2020. The Canadian Hydrological Model (CHM) v1.0: a multi-scale, multi-extent, variable-complexity hydrological model – design and overview. Geosci. Model Dev. 13, 225–247. https://doi.org/10.5194/gmd-13-225-2020.

Ménard, C.B., Essery, R., Pomeroy, J., 2014. Modelled sensitivity of the snow regime to topography, shrub fraction and shrub height. Hydrol. Earth Syst. Sc. 18, 2375–2392. https://doi.org/10.5194/hess-18-2375-2014.

Miller, M.H., Beauchamp, E.G., Lauzon, J.D., 1994. Leaching of Nitrogen and Phosphorus from the Biomass of Three Cover Crop Species. J. Environ. Qual. 23, 267–272. https://doi.org/10.2134/jeq1994.00472425002300020007x.

Mladenov, N., Williams, M.W., Schmidt, S.K., Cawley, K., 2012. Atmospheric deposition as a source of carbon and nutrients to an alpine catchment of the Colorado Rocky Mountains. Biogeosciences 9 (8), 3337–3355.

Monteith, J.L., 1965. Evaporation and environment. In: 19th Symposium of the Society for Experimental Biology. Cambridge University Press, Cambridge, pp. 205–234.

Munro, D., 2004. Revisiting bulk heat transfer on Peyto Glacier, Alberta, Canada, in light of the OG parameterization. J. Glaciol. 50 (171), 590–600. https://doi.org/10.3189/172756504781829819.

Nash, J.E., Sutcliffe, J.V., 1970. River flow forecasting through conceptual models. Part I – A discussion of principles. J. Hydrol. 10 (3), 282–290.

Naz, B.S., Frans, C.D., Clarke, G.K.C., Burns, P., Lettenmaier, D.P., 2014. Modeling the effect of glacier recession on streamflow response using a coupled glaciohydrological model. Hydrol. Earth Syst. Sc. 18, 787–802. https://doi.org/10.5194/hess-18-787-2014.

Nicholls, E.M., Carey, S.K., 2021. Evapotranspiration and energy partitioning across a forest-shrub vegetation gradient in a subarctic, alpine catchment. J. Hydrol. 602, 126790 https://doi.org/10.1016/j.jhydrol.2021.126790.

Nicholson, L., Benn, D., 2006. Calculating ice melt beneath a debris layer using meteorological data. J. Glaciol. 52 (178), 463–470. https://doi.org/10.3189/172756506781828584.

Oerlemans, J., Grisogono, B., 2002. Glacier winds and parameterisation of the related surface heat fluxes. Tellus A: Dyn. Meteorol. Oceanogr. 54, 440–452.

Östrem, G., 1959. Ice melting under a thin layer of moraine, and the existence of ice cores in moraine ridges. Geogr. Ann. 41 (4), 228–230. https://doi.org/10.1080/20014422.1959.11907953.

Pellerin, B.A., Saraceno, J.F., Shanley, J.B., Sebestyen, S.D., Aiken, G.R., Wollheim, W. M., Bergamaschi, B.A., 2012. Taking the pulse of snowmelt: In situ sensors reveal seasonal, event and diurnal patterns of nitrate and dissolved organic matter variability in an upland forest stream. Biogeochemistry 108 (1–3), 183–198.

Peters, N.E., Driscoll, C.T., 1987. Sources of acidity during snowmelt at a forested site in the west-central Adirondack Mountains, New York. Institute of Hydrology, IAHS Press 167, Wallingford, Oxfordshire, pp. 99 –108.

Plach, J.M., Macrae, M.L., Ali, G.A., Brunke, R.R., English, M.C., Ferguson, G., Van Esbroeck, C.J., 2018. Supply and Transport Limitations on Phosphorus Losses from Agricultural Fields in the Lower Great Lakes Region, Canada. J. Environ. Qual. 47, 96–105. https://doi.org/10.2134/jeq2017.06.0234.

Plüss, C., Ohmura, A., 1997. Longwave radiation on snow-covered mountainous surfaces. J. Appl. Meteorol. Clim. 36, 818–824. https://doi.org/10.1175/1520-0450-36.6.818.

Pomeroy, J.W., 1989. A process-based model of snow drifting. Ann. Glaciol. 13, 237–240.

Pomeroy, J.W., Gray, D.M., 1994. Sensitivity of snow relocation and sublimation to climate and surface vegetation, in: Jones, H.G., Davies, T. D., Ohmura, A., Morris E. M. (Eds.), Snow and Ice Covers: Interactions with Atmosphere and Ecosystems. IAHS Publication No. 223, IAHS Press, Wallingford, UK, pp. 213-226.

Pomeroy, J.W., Gray, D.M., 1995. Snowcover Accumulation, Relocation and Management, NHRI Science Report No. 7. Environment Canada, Saskatoon.

Pomeroy, J.W., Marks, D., Link, T.E., Ellis, C.R., Hardy, J., Rowlands, A., Granger, R.J., 2009. The impact of coniferous forest temperature on incoming longwave radiation to melting snow., Hydrol. Process. 23, 2513:2525, doi: 10.1002/hyp.7325.

Pomeroy, J., Fang, X., Shook, K., Westbrook, C., Brown, T., 2012b. Informing the Vermilion River Watershed Plan through Application of the Cold Regions Hydrological Model Platform, Centre for Hydrology Report No. 12. Centre for Hydrology, University of Saskatchewan, Saskatoon.

Pomeroy, J.W., Shook, K., Fang, X., Dumanski, S., Westbrook, C., Brown, T., 2014. Improving and testing the prairie hydrological model at Smith Creek Research Basin, Centre for Hydrology Report No. 14. Centre for Hydrology, University of Saskatchewan, Saskatoon.

Pomeroy, J.W., Fang, X., Rasouli, K., 2015. Sensitivity of snow processes to warming in the Canadian Rockies. in: Proceedings of the 72nd Eastern Snow Conference, 9–11 June 2015, Sherbrooke, Québec, Canada, pp. 22-33.

Pomeroy, J.W., Li, L., 2000. Prairie and arctic areal snow cover mass balance using a blowing snow model. J. Geophys. Res. 105, 26619–26634.

Pomeroy, J.W., Gray, D.M., Landine, P.G., 1993. The Prairie Blowing Snow Model: characteristics, validation, operation. J. Hydrol. 144, 165–192.

Pomeroy, J.W., Gray, D.M., Shook, K.R., Toth, B., Essery, R.L.H., Pietroniro, A., Hedstrom, N., 1998a. An evaluation of snow accumulation and ablation processes for land surface modelling. Hydrol. Process. 12 (15), 2339–2367.

Pomeroy, J.W., Parviainen, J., Hedstrom, N.R., Gray, D.M., 1998b. Coupled modelling of forest snow interception and sublimation. Hydrol. Process. 12 (15), 2317–2337.

Pomeroy, J.W., Male, D.H., 1992. Steady-state suspension of snow. J. Hydrol. 136, 275–301.

Pomeroy, J.W., Granger, R.J., Pietroniro, A., Toth, B., Hedstrom, N.R., 1999. Classification of the boreal forest for hydrological processes. In: Proceedings of 9th International Boreal Forest Research Association Conference, Oslo, Norway, pp. 49–59.

Pomeroy, J.W., Gray, D.M., 1990. Saltation of snow. Water Resour. Res. 26, 1583–1594.

Pomeroy, J.W., Essery, R.L.H., Toth, B., 2004. Implications of spatial distributions of snow mass and melt rate for snow-cover depletion: observations in a subarctic mountain catchment. Ann. Glaciol. 38, 195–201.
Pomeroy, J.W., Gray, D.M., Brown, T., Hedstrom, N.R., Quinton, W.L., Granger, R.J., Carey, S.K., 2007. The cold regions hydrological model: A platform for basing process representation and model structure on physical evidence. Hydrol. Process. 21, 2650–2667.
Pomeroy, J.W., Fang, X., Westbrook, C., Minke, A., Guo, X., Brown, T., 2010. Prairie Hydrological Model Study Final Report, Centre for Hydrology Report No. 7. Centre for Hydrology, University of Saskatchewan, Saskatoon.
Pomeroy, J.W., Fang, X., Ellis, C., 2012. Sensitivity of snowmelt hydrology in Marmot Creek, Alberta, to forest cover disturbance. Hydrol. Process. 26, 1891–1904. https://doi.org/10.1002/hyp.9248.
Pomeroy, J.W., Fang, X., Shook, K., Whitfield, P.H., 2013. Predicting in ungauged basins using physical principles obtained using the deductive, inductive, and abductive reasoning approach. In: Pomeroy, J.W., Whitfield, P.H., Spence, C. (Eds.), Putting Prediction in Ungauged Basins into Practice. Canadian Water Resources Association, Canada, pp. 41–62.
Pomeroy, J.W., Fang, X., Marks, D.G., 2016a. The cold rain-on-snow event of June 2013 in the Canadian Rockies – Characteristics and diagnosis. Hydrol. Process. 30 (17), 2899–2914. https://doi.org/10.1002/hyp.10905.
Pomeroy, J.W., Stewart, R.E., Whitfield, P.H., 2016b. The 2013 flood event in the Bow and Oldman River basins: causes, assessment and damages. Can. Water Resour. J. 41 (1–2), 105–117. https://doi.org/10.1080/07011784.2015.1089190.
Pradhananga, D., Pomeroy, J.W., 2022. Diagnosing changes in glacier hydrology from physical principles, using a hydrological model with snow redistribution, sublimation, firnification and energy balance ablation algorithms. J. Hydrol. 608, 127545 https://doi.org/10.1016/j.jhydrol.2022.127545.
Priestley, C.H.B., Taylor, R.J., 1972. On the assessment of surface heat flux and evaporation using large-scale parameters. Mon. Weather Rev. 100, 81–92.
Quinton, W.L., Baltzer, J.L., 2013. The active-layer hydrology of a peat plateau with thawing permafrost (Scotty Creek, Canada). Hydrogeol. J. 21 (1), 201–220. https://doi.org/10.1007/s10040-012-0935-2.
Quinton, W.L., Gray, D.M., 2001. Estimating subsurface drainage from organic covered hillslopes underlain by permafrost: toward a combined heat and mass flux model. In: Proceedings of IAHS Symposium on Soil, Vegetation, Atmosphere Transfer Schemes and Large Scale Hydrological Models during the 6th IAHS Scientific Assembly. IAHS Publication No. 270, Maastricht, Netherlands, pp. 333–341.
Rasouli, K., Pomeroy, J.W., Janowicz, J.R., Carey, S.K., Williams, T.J., 2014. Hydrological sensitivity of a northern mountain basin to climate change. Hydrol. Process. 28 (14), 4191–4208. https://doi.org/10.1002/hyp.10244.
Rasouli, K., Pomeroy, J.W., Whitfield, P.H., 2019. Hydrological responses of headwater basins to monthly perturbed climate in the North American Cordillera. J. Hydrometeorol. 20, 863–882. https://doi.org/10.1175/JHM-D-18-0166.1.
Rasouli, K., Pomeroy, J.W., Whitfield, P.H., 2022. The sensitivity of snow hydrology to changes in air temperature and precipitation in three North American headwater basins. J. Hydrol. 606, 127460 https://doi.org/10.1016/j.jhydrol.2022.127460.
Roste, J., 2015. Development and evaluation of a Canadian Prairie Nutrient Transport Model. M.Sc. thesis, University of Saskatchewan. Retrieved from http://hdl.handle.net/10388/ETD-2015-07-2172.
Sanmiguel-Vallelado, A., McPhee, J., Esmeralda Ojeda Carreño, P., Morán-Tejeda, E., Julio Camarero, J., López-Moreno, J.I., 2022. Sensitivity of forest–snow interactions to climate forcing: Local variability in a Pyrenean valley. J. Hydrol. 605, 127311 https://doi.org/10.1016/j.jhydrol.2021.127311.
Scherler, M., Hauck, C., Hoelzle, M., Stähli, M., Völksch, I., 2010. Meltwater infiltration into the frozen active layer at an alpine permafrost site. Permafr. Periglac. Process. 21 (4), 325–334. https://doi.org/10.1002/ppp.694.
Scherler, D., Wulf, H., Gorelick, N., 2018. Global assessment of supraglacial debris-cover extents. Geophys. Res. Lett. 45, 11798–11805. https://doi.org/10.1029/2018GL080158.
Schindler, D.W., Hecky, R.E., McCullough, G.K., 2012. The rapid eutrophication of Lake Winnipeg: Greening under global change. J. Great Lakes Res. 38 (Supplement 3), 6–13. https://doi.org/10.1016/j.jglr.2012.04.003.
Schuur, E., McGuire, A., Schädel, C., Grosse, G., Harden, J., Hayes, D.J., Vonk, J.E., 2015. Climate change and the permafrost carbon feedback. Nature 520, 171–179. https://doi.org/10.1038/nature14338.
Sebestyen, S.D., Boyer, E.W., Shanley, J.B., Kendall, C., Doctor, D.H., Aiken, G.R., Ohte, N., 2008. Sources, transformations, and hydrological processes that control stream nitrate and dissolved organic matter concentrations during snowmelt in an upland forest. Water Resour. Res. 44 (12), W12410. https://doi.org/10.1029/2008WR006983.
Shook, K.R., Gray, D.M., 1997. Synthesizing shallow seasonal snow covers. Water Resour. Res. 33, 419–426.
Shook, K., Papalexiou, S., Pomeroy, J.W., 2021. Quantifying the effects of prairie depressional storage complexes on drainage basin connectivity. J. Hydrol. 593, 125846 https://doi.org/10.1016/j.jhydrol.2020.125846.
Shook, K.R., Pomeroy, J.W., 2011a. Synthesis of incoming shortwave radiation for hydrological simulation. Hydrol. Res. 42, 433–446. https://doi.org/10.2166/nh.2011.074.
Shook, K.R., Pomeroy, J.W., 2011b. Memory effects of depressional storage in northern prairie hydrology. Hydrol. Process. 25 (25), 3890–3898.
Shook, K., Pomeroy, J.W., Spence, C., Boychuk, L., 2013. Storage dynamics simulations in prairie wetland hydrology models: evaluation and parameterization. Hydrol. Process. 27, 1875–1889. https://doi.org/10.1002/hyp.9867.
Shook, K., Pomeroy, J., van der Kamp, G., 2015. The transformation of frequency distributions of winter precipitation to spring streamflow probabilities in cold regions; case studies from the Canadian Prairies. J. Hydrol. 521, 395–409. https://doi.org/10.1016/j.jhydrol.2014.12.014.
Sicart, J.E., Pomeroy, J.W., Essery, R., Bewley, D.S., 2006. Incoming longwave radiation to melting snow: observations, sensitivity and estimation in northern environments. Hydrol. Process. 20, 3697–3708.
Skaggs, R.W., 1980. Drainmod Reference Report, Methods for Design and Evaluation of Drainage-Water Management Systems for Soils with High Water Tables. US Department of Agriculture, Soil Conservation Service, South National Technical Center, Fort Worth, Texas.
Smith, R.B., Bass, B., Sawyer, D., Depew, D., Watson, S.B., 2019. Estimating the economic costs of algal blooms in the Canadian Lake Erie Basin. Harmful Algae 87, 101624. https://doi.org/10.1016/j.hal.2019.101624.
Smith, V.H., Joye, S.B., Howarth, R.W., 2006. Eutrophication of Freshwater and Marine Ecosystem. Limnol. Oceanogr. 51, 351–355. https://doi.org/10.4319/lo.2006.51.1_part_2.0351.
Smith, C.D., 2009. The relationship between snowfall catch efficiency and wind speed for the Geonor T-200B precipitation gauge utilizing various wind shield configurations. In: Proceedings of 77th Western Snow Conference, pp. 115–121.
Snider, D.M., Wagner-Riddle, C., Spoelstra, J., 2017. Stable isotopes reveal rapid cycling of soil nitrogen after manure application. J. Environ. Qual. 46 (2), 261.
Spence, C., Woo, M., 2003. Hydrology of subarctic Canadian shield: soil filled valleys. J. Hydrol. 279 (1–4), 151–166.
Stone, L.E., Fang, X., Haynes, K.M., Helbig, M., Pomeroy, J.W., Sonnentag, O., Quinton, W.L., 2019. Modelling the effects of permafrost loss on discharge from a wetland-dominated, discontinuous permafrost basin. Hydrol. Process. 33, 2607–2626. https://doi.org/10.1002/hyp.13546.
Timmons, D.R., Holt, R.F., Latterell, J.J., 1970. Leaching of Crop Residues as a Source of Nutrients in Surface Runoff Water. Water Resour. Res. 6 (5), 1367–1375. https://doi.org/10.1029/WR006i005p01367.
Ulén, B., 1997. Nutrient losses by surface run-off from soils with winter cover crops and spring-ploughed soils in the south of Sweden. Soil Tillage Res. 44 (3–4), 165–177. https://doi.org/10.1016/S0167-1987(97)00051-2.
van der Kamp, G., Hayashi, M., 1998. The groundwater recharge function of small wetlands in the semi-arid northern prairies. Gr. Plains Res. 8, 39–56.
Van Esbroeck, C.J., Macrae, M.L., Brunke, R.I., McKague, K., 2016. Annual and seasonal phosphorus export in surface runoff and tile drainage from agricultural fields with cold temperate climates. J. Great Lakes Res. 42 (6), 1271–1280. https://doi.org/10.1016/j.jglr.2015.12.014.
Van Esbroeck, C.J., Macrae, M.L., Brunke, R.R., McKague, K., 2017. Surface and subsurface phosphorus export from agricultural fields during peak flow events over the nongrowing season in regions with cool, temperate climates. J. Soil Water Conserv. 72 (1), 65–76. https://doi.org/10.2489/jswc.72.1.65.
Van Hoy, D.F., Mahmood, T.H., Todhunter, P.E., Jeannotte, T.L., 2020. Mechanisms of cold region hydrologic change to recent wetting in a northern glaciated landscape. Water Resour. Res. 56, e2019WR026932. doi:10.1029/2019WR026932.
Verseghy, D.L., 1991. CLASS - A Canadian land surface scheme for GCMs, I. soil model. Int. J. Climatol. 11, 111–133.
Verseghy, D.L., McFarlane, N.A., Lazare, M., 1993. A Canadian land surface scheme for GCMs: II. Vegetation model and coupled runs. Int. J. Climatol. 13, 347–370.
Vionnet, V., Marsh, C.B., Menounos, B., Gascoin, S., Wayand, N.E., Shea, J., Mukherjee, K., Pomeroy, J.W., 2021. Multi-scale snowdrift-permitting modelling of mountain snowpack. The Cryosphere 15, 743–769. https://doi.org/10.5194/tc-15-743-2021.
Walmsley, J.L., Taylor, P.A., Salmon, J.R., 1989. Simple guidelines for estimating windspeed variations due to small-scale topographic features – an update. Climatol. Bull. 23 (1), 3–14.
Walvoord, M.A., Kurylyk, B.L., 2016. Hydrologic Impacts of Thawing Permafrost—A Review. Vadose Zone J. 15 (6) https://doi.org/10.2136/vzj2016.01.0010.
Weber, M., Bernhardt, M., Pomeroy, J.W., Fang, X., Härer, S., Schulz, K., 2016. Description of current and future snow processes in a small basin in the Bavarian Alps Environ. Environ. Earth Sci. 75, 1223. https://doi.org/10.1007/s12665-016-6027-1.
Weedon, G.P., Balsamo, G., Bellouin, N., Gomes, S., Best, M.J., Viterbo, P., 2014. The WFDEI meteorological forcing data set: WATCH Forcing Data methodology applied to ERA-Interim reanalysis data. Water Resour. Res. 50 (9), 7505–7514. https://doi.org/10.1002/2014WR015638.
Wheater, H.S., Pomeroy, J.W., Pietroniro, A., Davison, B., Elshamy, M., Yassin, F., Bahrami, A., 2022. Advances in modelling large river basins in cold regions with Modélisation Environmentale Communautaire—Surface and Hydrology (MESH), the Canadian hydrological land surface scheme. Hydrol. Process. 36 (4), e14557. https://doi.org/10.1002/hyp.14557.
White, E.M., 1973. Water-Leachable Nutrients from Frozen or Dried Prairie Vegetation. J. Environ. Qual. 2, 104–107. https://doi.org/10.2134/jeq1973.00472425000200010015x.
Williams, T.J., Pomeroy, J.W., Janowicz, J.R., Carey, S.K., Rasouli, K., Quinton, W.L., 2015. A radiative–conductive–convective approach to calculate thaw season ground surface temperatures for modelling frost table dynamics. Hydrol. Process. 29 (18), 3954–3965. https://doi.org/10.1002/hyp.10573.
Woo, M.-k., Arain, M.A., Mollinga, M., Yi, S., 2004. A two-directional freeze and thaw algorithm for hydrologic and land surface modelling. Geophys. Res. Lett. 31 (12), 1–4. https://doi.org/10.1029/2004GL019475.
Woo, M.-K., Pomeroy, J., 2012. Snow and Runoff: Processes, Sensitivity and Vulnerability. In: French, H., Slaymaker, O. (Eds.), Changing Cold Environments: A Canadian Perspective. John Wiley & Sons Ltd, Chichester, UK, pp. 105–125. https://doi.org/10.1002/9781119950172.ch6.

Woo, M.-k., Mollinga, M., Smith, S.L., 2007. Climate warming and active layer thaw in the boreal and tundra environments of the Mackenzie Valley. Can. J. Earth Sci. 44 (6), 733–743. https://doi.org/10.1139/e06-121.

Xie, C., Gough, W.A., 2013. A simple thaw-freeze algorithm for multi-layered soil using the Stefan equation. Permafr. Periglac. Process. 24, 252–260. https://doi.org/10.1002/ppp.1770.

Zhang, X.B., Vincent, L.A., Hogg, W.D., Niitsoo, A., 2000. Temperature and precipitation trends in Canada during the 20th Century. Atmos. Ocean 38, 395–429.

Zhao, L., Gray, D.M., 1999. Estimating snowmelt infiltration into frozen soils. Hydrol. Process. 13 (12-13), 1827-1842.

Zhao, L.T., Gray, D.M., 1997. A parametric expression for estimating infiltration into frozen soils. Hydrol. Process. 11 (13), 1761–1775.

Zhao, L.T., Gray, D.M., Male, D.H., 1997. Numerical analysis of simultaneous heat and mass transfer during infiltration into frozen ground. J. Hydrol. 200, 345–363.

Zhou, J., Pomeroy, J.W., Zhang, W., Cheng, G., Wang, G.X., Chen, C., 2014. Simulating cold regions hydrological processes using a modular model in the west of China. J. Hydrol. 509, 13–24. https://doi.org/10.1016/j.jhydrol.2013.11.013.

Further reading

Spence, Chris, He, Zhihua, Shook, Kevin, Pomeroy, John, Whitfield, Colin, Wolfe, Jared, 2022. Assessing runoff sensitivity of North American Prairie Pothole Region basins to wetland drainage using a basin classification-based virtual modelling approach. Hydrology and Earth System Science 26 (21), 5555–5575. https://doi.org/10.5194/hess-26-5555-2022.